Astronomy & Astrophysics manuscript no. 11533
June 16, 2009

Searching for a link between the magnetic nature and other observed properties of Herbig Ae/Be stars and stars with debris disks⋆

S. Hubrig[1,2], B. Stelzer[3], M. Schöller[4], C. Grady[5], O. Schütz[2], M. A. Pogodin[6,7], M. Curé[8], K. Hamaguchi[9], and R. V. Yudin[6,7]

[1] Astrophysikalisches Institut Potsdam, An der Sternwarte 16, 14482 Potsdam, Germany
[2] European Southern Observatory, Casilla 19001, Santiago 19, Chile
[3] INAF-Osservatorio Astronomico di Palermo, Piazza del Parlamento 1, 90134 Palermo, Italy
[4] European Southern Observatory, Karl-Schwarzschild-Str. 2, 85748 Garching, Germany
[5] Eureka Scientific, 2452 Delmer, Suite 100, Oakland, CA 96002, USA
[6] Pulkovo Observatory, Saint-Petersburg, 196140, Russia
[7] Isaac Newton Institute of Chile, Saint-Petersburg Branch, Russia
[8] Departamento de Física y Astronomía, Facultad de Ciencias, Universidad de Valparaíso, Chile
[9] Astrophysics Science Division, NASA's Goddard Space Flight Center, Greenbelt, MD 20771, USA

Received date / Accepted date

ABSTRACT

Context. Recently, evidence for the presence of weak magnetic fields in Herbig Ae/Be stars has been found in several studies.

Aims. We seek to expand the sample of intermediate-mass pre-main sequence stars with circular polarization data to measure their magnetic fields, and to determine whether magnetic field properties in these stars are correlated with mass-accretion rate, disk inclination, companions, silicates, PAHs, or show a correlation with age and X-ray emission as expected for the decay of a remnant dynamo.

Methods. Spectropolarimetric observations of 21 Herbig Ae/Be stars and six debris disk stars have been obtained at the European Southern Observatory with FORS 1 mounted on the 8 m Kueyen telescope of the VLT. With the GRISM 600B in the wavelength range 3250–6215 Å we were able to cover all hydrogen Balmer lines from Hβ to the Balmer jump. In all observations a slit width of $0\farcs4$ was used to obtain a spectral resolving power of $R \approx 2000$.

Results. Among the 21 Herbig Ae/Be stars studied, new detections of a magnetic field were achieved in six stars. For three Herbig Ae/Be stars, we confirm previous magnetic field detections. The largest longitudinal magnetic field, $\langle B_z \rangle = -454 \pm 42$ G, was detected in the Herbig Ae/Be star HD 101412 using hydrogen lines. No field detection at a significance level of 3σ was achieved in stars with debris disks. Our study does not indicate any correlation of the strength of the longitudinal magnetic field with disk orientation, disk geometry, or the presence of a companion. We also do not see any simple dependence on the mass-accretion rate. However, it is likely that the range of observed field values qualitatively supports the expectations from magnetospheric accretion models giving support for dipole-like field geometries. Both the magnetic field strength and the X-ray emission show hints of a decline with age in the range of ∼2–14 Myrs probed by our sample, supporting a dynamo mechanism that decays with age. However, our study of rotation does not show any obvious trend of the strength of the longitudinal magnetic field with rotation period. Furthermore, the stars seem to obey the universal power-law relation between magnetic flux and X-ray luminosity established for the Sun and main-sequence active dwarf stars.

Key words. polarization - Stars: pre-main-sequence - Stars: circumstellar matter - Stars: magnetic fields - Xrays: stars - Stars: coronae - Stars: activity

1. Introduction

Magnetic fields are important ingredients of the star formation process (McKee & Ostriker 2007). Models of magnetically driven accretion and outflows (e.g., Shu et al. 2000; Shu et al. 1995) successfully reproduce many observational properties of low-mass pre-main sequence stars, the classical T Tauri stars (cTTS). Indirect observational evidence for the presence of magnetic fields in these stars is seen in strong X-ray, FUV, and UV emission (e.g., Feigelson & Montmerle 1999; Brown et al. 1985). The high-energy radiation of young stars related to magnetic processes may be critical for the annealing and melting of some refractory grain species (Shu et al. 2001), for the heating intermediate-depth portions of disks around young stars (Najita 2004) and for mass loss from planets forming in those disks (Penz et al. 2008). The irradiation-induced heating mediated by the magnetic activity enlarges the zone in circumstellar disks where chemistry may proceed to assemble prebiotic materials which could produce life-bearing worlds. Therefore, understanding the interaction between central

⋆ Based on observations obtained at the European Southern Observatory, Paranal, Chile (ESO programmes 077.C-0521(A) and 081.C-0410(A)).

stars, their magnetic fields and protoplanetary disks is crucial to reconstruct the Solar System's history, and to account for the diversity of exo-planetary systems.

Direct magnetic field measurements of cTTS (e.g. Johns-Krull 2007) corroborate the scenario outlined above for the formation of low-mass stars, but the picture is less clear for higher-mass stars. The presence of protoplanetary disks around intermediate-mass pre-main sequence (PMS) stars, the Herbig Ae/Be stars (e.g., Herbig 1960; Finkenzeller & Mundt 1984; Thé et al. 1994), has been established through their thermal emission in the IR, and more recently by direct imaging with polarimetric and interferometric techniques (e.g., Perrin et al. 2004; Monnier et al. 2005). Dusty disk models explain the IR excess emission (e.g. Dullemond et al. 2001) and magnetospheric accretion models describe the line profiles of Herbig Ae/Be stars (Muzerolle et al. 2004), in close analogy to cTTS. However, the disk lifetime appears to be shorter for Herbig Ae/Be stars (Uzpen et al. 2009; Carpenter et al. 2005) and within the Herbig Ae/Be class there is a trend of more massive stars dispersing their disks more rapidly (Alonso-Albi et al. 2009). Herbig Ae stars are closer analogs to TTS than Herbig Be stars. Bipolar outflows or associated Herbig-Haro knots are now known for six optically visible Herbig Ae stars drawn from coronographic imaging surveys (e.g. Melnikov et al. 2008). Due to the probable role of magnetic fields in launching and collimating jets, this implies that a significant fraction of Herbig Ae stars should have measurable magnetic fields, which could persist through much, if not all, of the star's PMS lifetime. X-ray activity is known for a number of Herbig Ae stars (Hamaguchi et al. 2005; Feigelson et al. 2003; Swartz et al. 2005; Stelzer et al. 2006, 2009; Skinner et al. 2004), suggesting the presence of magnetic fields. Recent advances in instrumentation have resulted in the first magnetic field measurements for Herbig Ae stars, derived from spectropolarimetry. A few stars have magnetic field strengths derived from circular polarization measurements of a few hundred Gauss or near 100 G (Hubrig et al. 2004a; Wade et al. 2005, 2007; Hubrig et al. 2006a, 2007a). Other objects seem to have either smaller average field strengths, or exhibit significant variability.

In our previous studies, we reported detections at a level higher than 3σ for three out of seven Herbig Ae stars observed with FORS 1 (Hubrig et al. 2004a, 2006a, 2007a). The results of the spectropolarimetric observations of the two Herbig Ae stars HD 31648 and HD 190073 with FORS 1 at a resolution of $R \approx 4000$ turned out to be especially remarkable (Hubrig et al. 2006a; Hubrig et al. 2007a). These two stars possess almost the same effective temperature, but are different in luminosity and projected rotation velocity. In the Stokes V spectra of HD 190073, the profiles exhibit a number of blueshifted local absorption components, whereas in HD 31648, only one blueshifted and one redshifted feature are observed in both H&K lines of the Ca II doublet. It is noteworthy that recent Goddard Fabry-Perot narrow band images revealed the counterjet and bright HH knots in HD 31648 (Stecklum et al. 2009, in preparation). This star demonstrates notable emission in the Hβ, Hγ, and Hδ lines, which indicates the presence of a significant stellar wind. The profiles of these lines are of P Cyg-type with very deep blueshifted absorptions.

In this work we seek to expand the sample of intermediate-mass PMS stars with circular polarization data used to derive stellar magnetic fields. We then investigate whether the magnetic field properties of these stars are correlated with mass-accretion rate, companions, silicates, or PAHs. We also search for the first time for a correlation between field strength and age or X-ray emission, such as expected for a decaying fossil field. Further, we examine the inclination dependence of the polarization data, and explore the dependence of the strength of the longitudinal magnetic field on stellar rotation.

2. Observations and data reduction

The observations reported here were carried out on May 22 and 23, 2008 in visitor mode at the European Southern Observatory with FORS 1 mounted on the 8 m Kueyen telescope of the VLT. This multi-mode instrument is equipped with polarisation analyzing optics comprising super-achromatic half-wave and quarter-wave phase retarder plates, and a Wollaston prism with a beam divergence of $22''$ in standard resolution mode. In 2007, a new mosaic detector with blue optimized E2V chips was installed in FORS 1. It has a pixel size of 15 μm (compared to 24 μm for the previous Tektronix chip) and a higher efficiency in the wavelength range below 6000 Å. To achieve the highest possible signal-to-noise (S/N) ratio – as is required for accurate measurements of stellar magnetic fields – we used the (200kHz, low, 1×1) readout mode, which makes it possible to achieve a S/N ratio of about 1000–1200 with only one single exposure. With the GRISM 600B in the wavelength range 3250–6215 Å we were able to cover all hydrogen Balmer lines from Hβ to the Balmer jump. In all observations, a slit width of $0\farcs4$ was used to obtain a spectral resolving power of $R \approx 2000$. Usually, we took three to five continuous series of two exposures for each object, leading to signal-to-noise ratios of typically 3000 to 4000. For the faintest Herbig Ae star in our sample, VV Ser, only two series were taken due to the rather long exposure time for each sub-exposure. More details on the observing technique with FORS 1 can be found elsewhere (e.g., Hubrig et al. 2004a, 2004c, and references therein).

The mean longitudinal magnetic field is the average over the stellar hemisphere visible at the time of observation of the component of the magnetic field parallel to the line of sight, weighted by the local emergent spectral line intensity. Its determination is based on the use of the equation

$$\frac{V}{I} = -\frac{g_{\rm eff} e \lambda^2}{4\pi m_e c^2} \, \frac{1}{I} \, \frac{{\rm d}I}{{\rm d}\lambda} \, \langle B_z \rangle \, , \qquad (1)$$

where V is the Stokes parameter which measures the circular polarization, I is the intensity observed in unpolarized light, $g_{\rm eff}$ is the effective Landé factor, e is the electron charge, λ is the wavelength, m_e the electron mass, c the speed of light, ${\rm d}I/{\rm d}\lambda$ is the derivative of Stokes I, and $\langle B_z \rangle$ is the mean longitudinal magnetic field. To minimize the cross-talk effect, we executed the sequence +45−45, +45−45, +45−45 etc. and calculated the values V/I using:

$$\frac{V}{I} = \frac{1}{2} \left\{ \left(\frac{f^{\rm o} - f^{\rm e}}{f^{\rm o} + f^{\rm e}} \right)_{\alpha=-45^\circ} - \left(\frac{f^{\rm o} - f^{\rm e}}{f^{\rm o} + f^{\rm e}} \right)_{\alpha=+45^\circ} \right\} , \qquad (2)$$

where α denotes the position angle of the retarder waveplate and $f^{\rm o}$ and $f^{\rm e}$ are ordinary and extraordinary beams,

respectively. Stokes I values were obtained from the sum of the ordinary and extraordinary beams, which are recorded simultaneously by the detector. To derive $\langle B_z \rangle$, a least-squares technique was used to minimize the expression

$$\chi^2 = \sum_i \frac{(y_i - \langle B_z \rangle\, x_i - b)^2}{\sigma_i^2} \quad (3)$$

where, for each spectral point i, $y_i = (V/I)_i$, $x_i = -\frac{g_{\rm eff} e \lambda_i^2}{4\pi m_e c^2}\,(1/I \times {\rm d}I/{\rm d}\lambda)_i$, and b is a constant term that, assuming that Eq. 1 is correct, approximates the fraction of instrumental polarization not removed after the application of Eq. 2 to the observations. During the commissioning of FORS 1, this instrumental polarization term was found to be wavelength independent. We assume that the only source of uncertainty in our field measurements is from the photon count statistics of the observations. Therefore, the longitudinal field uncertainty is obtained from the formal uncertainty of the linear regression. For each spectral point i, the derivative of Stokes I with respect to the wavelength was evaluated following

$$\left(\frac{{\rm d}I}{{\rm d}\lambda}\right)_{\lambda=\lambda_i} = \frac{N_{i+1} - N_{i-1}}{\lambda_{i+1} - \lambda_{i-1}}, \quad (4)$$

where N_i is the photon count at wavelength λ_i. Since noise strongly influences the derivative, we interpolate the data after spectrum extraction with splines. Our experience from a study of a large sample of magnetic and non-magnetic Ap and Bp stars (Hubrig et al. 2006b) revealed that this regression technique is very robust and that detections with $\langle B_z \rangle \geq 3\sigma$ result only for stars possessing magnetic fields.

The list of the studied stars is presented in Table 1. In the four columns we give the object name, another identifier from SIMBAD, the visual magnitude and the spectral type. The star HD 47839 of spectral type O7 V was included in our sample since it is classified as a pre-main sequence star in the SIMBAD database, probably due to its close proximity to the Cone Nebula. Markova et al. (2004) consider this star as a Galactic O-type star with a mass of 32 $M_\odot$ and $T_{\rm eff}$=37 500 K. In Table 2 we list various properties of the studied stars compiled from the literature, such as $v \sin i$, mass-accretion rate, features in the mid-IR spectra, the presence of a companion, effective temperature, luminosity, and age. The mass was deduced from the position of the star in the H-R diagram (see Sect. 5). The mass-accretion rates were determined by Garcia Lopez et al. (2006) from the luminosity of the Brγ line seen in emission in Herbig Ae/Be stars. Mid-IR features such as crystalline silicate grains indicate thermal dust processing subsequent to the formation of the star-disk system, while PAHs (polycyclic aromatic hydrocarbons) are abundant in interstellar and circumstellar environments and can be important constituents in the energy balance of those environments as sources of photoelectrons that heat the gas component (Kamp & Dullemond 2004). Since the existence of a link between the presence of magnetic fields and the disk characteristics remains unproven, we decided to include in this study also the information on mid-IR features. Additionally, in Tables 1 and 2 we added five Herbig Ae/Be stars for which magnetic fields were detected in previous studies by various authors. The magnetic field for HD 31648 was detected by Hubrig et al. (2006b), while V380 Ori and BF Ori were studied by Wade et al. (2005). The detection of a weak magnetic field in HD 104237 was reported by Donati et al. (1997) and the study of the magnetic field of HD 200775 was carried out by Alecian et al. (2008). We note, however, that, as was shown by Hubrig et al. (2007b), the detected magnetic field of HD 31648 is predominantly circumstellar (CS) and that the strength of the photospheric magnetic field remains unknown. Also, the field detection in HD 104237 of the order of ∼50 G was just marginal, and was not confirmed in the follow-up study by Wade et al. (2007).

Since caution is called for in the detection of magnetic fields with low resolution spectropolarimeters, from time to time we observed magnetic Ap/Bp stars with well-known variation curves. These observations confirm that our measurements are usually in good agreement with measurements obtained with other spectropolarimeters (see e.g. Hubrig et al. 2004b). During our observing run, we also observed the A-type star HD 162725, for which previous measurements exist both with FORS 1 and later with ESPaDOnS at the Canada-France-Hawaii Telescope at much higher spectral resolution (R=65 000). Due to lack

Table 1. Target stars for which spectropolarimetric data were obtained during our observing run.

Object name	Other identifier	V	Spectral type
PDS 2	CPD−53 295	10.7	F2
HD 47839	15 Mon	4.7	O7 Ve
HD 95881	Hen 3-554	8.3	A1 III
HD 97048	CU Cha	8.5	A0pshe
HD 97300	CED 112 IRS 3	9.0	B9 V
HD 100453	CD-53 4102	7.8	A9 Ve
HD 100546	KR Mus	6.7	B9 Vne
HD 101412	V1052 Cen	9.0	B9.5 V
HD 135344B	SAO 206462	7.8	F4–F8
HD 139614	Hen 3-1086	8.3	A7 Ve
HD 144432	Hen 3-1141	8.2	A9/F0 V
HD 144668	HR 5999	7.0	A7 IVe
HD 150193	V2307 Oph	8.9	A1 Ve
HD 152404	AK Sco	9.1	F5 Ve
HD 158643	51 Oph	4.8	A0 V
HD 163296	MWC 275	6.9	A1 Ve
HD 169142	MWC 925	8.2	B9 Ve
VV Ser	FMC 39	11.6	A2e
HD 176386	CD−37 13023	7.3	B9 IVe
HD 179218	BD+15 1991	7.2	B9e
HD 190073	MWC 325	7.8	A2 IVpe
Stars with debris disks			
HD 9672	49 Cet	5.6	A1 V
HD 39060	β Pic	3.9	A6V
HD 109573	HR 4796	5.8	A0 V
HD 164249	CD-51 11312	7.3	F5 V
HD 172555	HR 7012	4.8	A7 V
HD 181327	CD-54 8270	7.0	F5/F6V
Magnetic Herbig Ae/Be stars from previous studies			
HD 31648	MWC 480	7.7	A3pshe
HD 104237	Hen 3-741	6.6	A:pe
HD 200775	MWC 361	7.4	B2 Ve
V380 Ori	MWC 765	10.7	A0
BF Ori	BD−061259	10.3	A5II/IIIev
Standard Ap star with a weak magnetic field			
HD 162725	V951 Sco	6.4	Ap

Notes: Spectral types and visual magnitudes are taken from SIMBAD.

Table 2. Targets discussed in this paper.

Object name	$v \sin i$ [km s^{-1}]	log $\dot{M}_{\rm acc}$ [$M_\odot$/yr]	IR feature	Comp.	log $T_{\rm eff}$ [K]	log L [$L_\odot$]	M [$M_\odot$]	age [Myr]
PDS 2	175[a]			no	3.98[d]	1.68[d]	2.5	
HD 47839*	120[b]			yes[ee]	4.57[uu]	5.23[uu]		$\sim$0.3[eee]
HD 95881	50[c]	-8.04	Si, PAH[r]	yes[ff]	3.86[vv]	1.84[vv]	3.1	>3[x]
HD 97048	140[d]	-7.17	PAH[s]	no[gg]	4.00[s]	1.64[s]	2.5	>2[d]
HD 97300		<-8.18	PAH[t]	yes[hh]	4.02[ww]	1.54[ww]	2.5	>3[ww]
HD 100453	39[e]	-8.04	PAH[u]	yes[ii]	3.87[s]	0.90[s]	1.7	14 ± 4[x]
HD 100546	65[f]		Si, PAH[u]	no[gg]	4.02[s]	1.51[s]	2.5	>10[d]
HD 101412	5[g]		Si, PAH[v]	yes[gg]	3.98[xx]	1.74[xx]	2.5	~2[fff]
HD 135344B	69[h]	-8.27	Si[s], PAH[w]	yes[jj]	3.82[s]	0.91[s]	1.6	8 ± 4[x]
HD 139614	15[i]	-7.99	Si[u]	yes[ee]	3.90[s]	0.91[s]	1.8	>10[x]
HD 144432	70[i]	-7.07	Si[u]	yes[kk]	3.87[s]	1.01[s]	1.8	10 ± 5[x]
HD 144668	100[i]	-6.37	Si[x]	yes[ll]	3.90[s]	1.94[s]	3.1	0.6 ± 0.4[ww]
HD 150193	100[f]	-7.29	Si[s]	yes[mm]	3.95[s]	1.38[s]	2.2	>2[d]
HD 152404	18.5[j]		Si[y]	yes[j]	3.81[s]	0.95[s]	1.7	~8[vv]
HD 158643	267[h]/228[k]	-6.87	Si[u]	no[nn]	4.00[d]	2.39[d]	3.9	0.3[d]
HD 163296	130[i]	-7.12	Si[u]	no[gg]	3.94[s]	1.38[s]	2.2	5 ± 2[x]
HD 169142	66[h]	-7.40	PAH[w]	yes[oo]	3.91[s]	1.16[s]	2.0	6 ± 3[x]
VV Ser	142[a]/229[l]	-6.34	Si[z]	no[gg]	3.95[s]	1.27[s]	2.0	3.5 ± 0.5[ggg]
HD 176386		-8.11	PAH[aa]	yes[ee]	4.03[ww]	1.69[ww]	2.7	>2[ww]
HD 179218	60[b]	-6.59	Si, PAH[u]	no[gg]	4.02[s]	2.00[s]	3.0	1.3 ± 0.5[x]
HD 190073	12[i]		Si, PAH[r]	yes[ff]	3.95[d]	1.80[d]	2.7	1.2 ± 0.6[hhh]
Stars with debris disks								
HD 9672	196[k]		_[bb]	no	4.00[yy]	1.42[yy]	2.3	~8[iii]
HD 39060	130[m]		Si[cc]	no	3.91[zz]	0.95[zz]	1.8	~12[jjj]
HD 109573	152[k]	<-8.53	_[bb]	yes[pp]	3.97[aaa]	1.32[aaa]	2.2	8 ± 2[pp]
HD 164249				yes[qq]	3.81[bbb]	0.48[n]	1.4	~12[jjj]
HD 172555			Si[dd]	no	3.89[bbb]	0.96[n]	1.7	~12[jjj]
HD 181327	16[n]			no	3.81[bbb]	0.54[n]	1.4	~12[jjj]
Magnetic Herbig Ae/Be stars from previous studies								
HD 31648*	90[o]		Si[s]	no[rr]	3.94[s]	1.14[s]	2.0	~7[kkk]
HD 104237*	10[h]	-7.45	Si[s]	yes[ss]	3.93[s]	1.54[s]	2.2	2.0 ± 0.5[ww]
HD 200775*	26[p]			yes[tt]	4.29[s]	3.82[s]		0.1 ± 0.05[ww]
V380 Ori	200[f]		Si[x]	yes[ee]	3.97[d]	2.04[ddd]	3.0	1.5 ± 0.5[x]
BF Ori	37[l]		Si[s]	no	3.95[s]	1.53[s]	2.3	~2[lll]
Standard Ap star with a weak magnetic field								
HD 162725	32[q]				3.99[ccc]	2.33[ccc]		

Notes: The information on $v \sin i$ values, mass-accretion rate, IR features, binarity, effective temperature, luminosity, and age was collected from the literature. The mass was deduced from the position of the star in the H-R diagram (see Sect. 5). Objects marked with * are excluded from the correlation analysis (see Sects. 2, 4.3, and 5.1).
References: [a]Vieira et al. (2003), [b]Bernacca & Perinotto (1970), [c]Grady et al. (1996), [d]van den Ancker et al. (1998), [e]Acke & Waelkens (2004), [f]Hamidouche et al. (2008), [g]this work, [h]Dunkin et al. (1997), [i]Hubrig et al. (2007b), [j]Alencar et al. (2003), [k]Royer et al. (2007), [l]Mora et al. (2001), [m]Slettebak (1982), [n]de la Reza & Pinzón (2004), [o]Beskrovnaya et al. (2004), [p]Alecian et al. (2008), [q]Landstreet et al. (2008), [r]Boersma et al. (2008), [s]Acke & van den Ancker (2004), [t]Siebenmorgen et al. (1998), [u]Meeus et al. (2001), [v]Geers et al. (2007), [w]Sloan et al. (2005), [x]van Boekel et al. (2005), [y]Przygodda et al. (2003), [z]Pontoppidan et al. (2007b), [aa]Siebenmorgen et al. (2000), [bb]Kessler-Silacci et al. (2005), [cc]Okamoto et al. (2004), [dd]Schütz et al. (2005b), [ee]Dommanget & Nys (1994), [ff]Baines et al. (2006), [gg]Corporon & Lagrange (1999), [hh]Stelzer et al. (2006), [ii]Chen et al. (2006a), [jj]Augereau et al. (2001), [kk]Carmona et al. (2007), [ll]Stecklum et al. (1995), [mm]Reipurth & Zinnecker (1993), [nn]Roberge et al. (2002), [oo]Grady et al. (2007), [pp]Stauffer et al. (1995), [qq]SIMBAD, [rr]Eisner et al. (2004), [ss]Grady et al. (2004), [tt]Pirzkal et al. (1997), [uu]Schnerr et al. (2007), [vv]Blondel et al. (2006), [ww]van den Ancker et al. (1997), [xx]Wade et al. (2007), [yy]Hughes et al. (2008), [zz]di Folco et al. (2004), [aaa]Debes et al. (2008), [bbb]Zuckerman & Song (2004), [ccc]Folsom et al. (2007), [ddd]Corcoran & Ray (1998), [eee]Walsh (1980), [fff]Wade et al. (2005), [ggg]Pontoppidan et al. (2007a), [hhh]Catala et al. (2007), [iii]Thi et al. (2001), [jjj]Zuckerman et al. (2001), [kkk]Simon et al. (2000), and [lll]Natta et al. (1997).

of time we obtained only three series of two exposures, resulting in a magnetic field measurement $\langle B_{\rm z} \rangle = 128 \pm 30$ G using the full spectrum and $\langle B_{\rm z} \rangle = 158 \pm 38$ G using hydrogen lines. This star was previously observed by Bagnulo et al. (2006), who failed to detect a magnetic field in this star. The non-detection by these authors is probably due to the much lower spectral resolution in their spectropolarimetric observations with FORS 1 (with a slit width of 0.″5–1.″0). Landstreet et al. (2008) detected a weak magnetic field of the order of -100 G with ESPaDOnS, and could also show

that the field is variable. We confirm their finding with our result, revealing a positive magnetic field of the order of 130–160 G, measured in metal and hydrogen lines (see Table 3). We note, however, that an accurate ephemeris for HD 162725 is not known and presently it is not possible to prove whether our observations were carried out in the opposite rotational phase compared to the observations of Landstreet et al. (2008).

Certainly, the advantage of using high resolution spectropolarimeters such as ESPaDOnS at the Canada-France-Hawaii Telescope, and NARVAL at the Bernard Lyot Telescope at Pic du Midi Observatory (France) is indubitable, since higher spectral resolution observations provide more detailed information about the behaviour of different elements in the presence of a magnetic field and on the magnetic field topology. On the other hand, the use of hydrogen lines, which are usually not used for magnetic field measurements with ESPaDOnS and NARVAL, offers the unique opportunity to study the global structure of the detected magnetic field. The profiles of metal lines frequently exhibit conspicuous variations, which are signatures of the circumstellar environment, stellar winds, of a non-uniform distribution of metals over the stellar surface, or of the presence of temperature spots (which are typical for late type stars). In our studies with FORS 1, the longitudinal magnetic fields are measured in two ways: using only the absorption hydrogen Balmer lines or using the whole spectrum including all available absorption lines, i.e. we use all lines, variable and non-variable, together. As hydrogen is expected to be homogeneously distributed over the stellar surface, the longitudinal magnetic field measurements sample the magnetic field fairly uniformly over the observed hemisphere.

3. Results

The obtained magnetic field measurements are presented in Table 3. In the first two columns, we give the object name of the targets and the modified Julian dates of the middle of the exposures. In the third column we list the signal-to-noise ratio (SNR) calculated in the final one-dimensional spectrum around 4750 Å. The measured mean longitudinal magnetic field $\langle B_{\rm z}\rangle$ using all absorption lines is presented in Col. 4. The measured mean longitudinal magnetic field $\langle B_{\rm z}\rangle$ using all hydrogen lines in absorption is listed in Col. 5. All quoted errors are 1σ uncertainties. In Col. 6, we identify new detections by ND and confirmed detections by CD. We note that all claimed detections have a significance of at least 3σ, determined from the formal uncertainties we derive. These measurements are indicated in bold face. In Figure 1 we show the significance distributions of our measurements. These distributions are different from the distribution shown by Wade et al. (2007) for their sample of FORS 1 observations of Herbig Ae/Be stars. Assuming that only formal uncertainties apply, this suggests that the Herbig stars in our sample are probably weakly magnetic.

Apart from the confirmed detections of a magnetic field in the stars HD 101412, HD 144668, and HD 190073 (Wade et al. 2007; Hubrig et al. 2007b; Catala et al. 2007), six other stars of our sample, PDS 2, HD 97048, HD 100546, HD 135344, HD 150193, and HD 176386, show evidence for the presence of a weak magnetic field. About half of the stars with magnetic field detections possess longitudinal magnetic fields larger than 100 G. These stars are the best

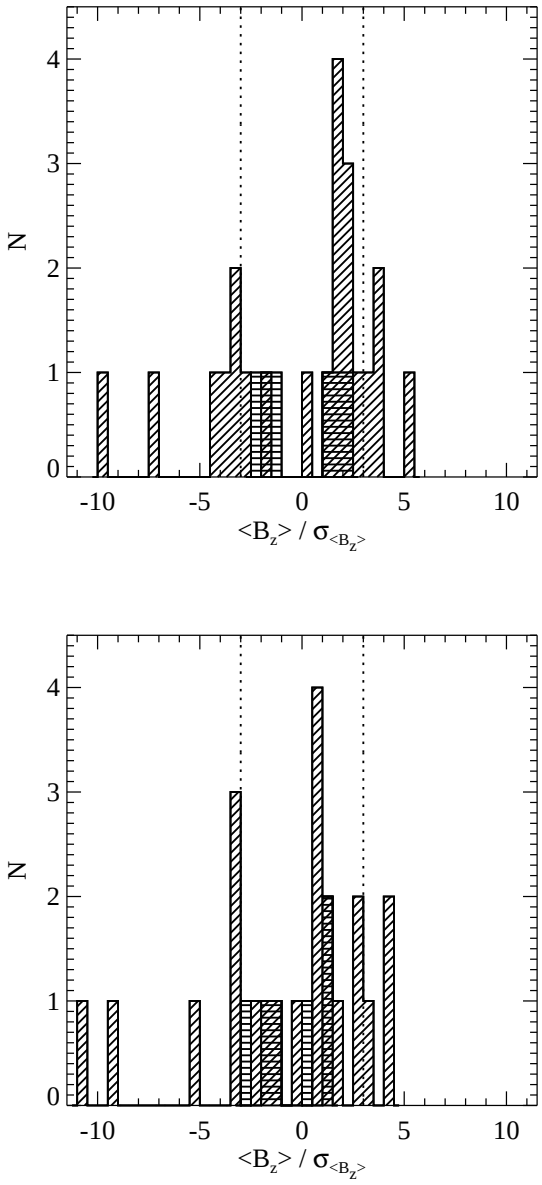

Fig. 1. Distribution of the detection significance $\langle B_{\rm z}\rangle/\sigma_{\langle B_{\rm z}\rangle}$ for our programme stars. Diagonal lines denote the Herbig Ae/Be stars, while horizontal lines denote the debris disk stars. Top: Results using the full spectra (Col. 4 of Table 3). Bottom: Results using only the hydrogen Balmer lines (Col. 5 of Table 3).

candidates for future spectropolarimetric studies to analyze the behaviour of their magnetic fields over their rotational cycles to disclose the magnetic topology of their surfaces. For two Herbig Ae stars, HD 139614 and HD 144432, with previously detected weak magnetic fields at a significance level of 3σ (Hubrig et al. 2004b; Hubrig et al. 2007b), the magnetic field in the present study was diagnosed only at a level of 1.8σ and 1.6σ, respectively. Wade et al. (2005) failed to detect a magnetic field in HD 139614 with quoted uncertainties of 25 G on two consecutive nights with the high resolution spectropolarimeter ESPaDOnS. The marginal de-

Table 3. The mean longitudinal magnetic field measurements for our sample of Herbig Ae/Be and debris disk stars observed with FORS 1.

Object name	MJD	SNR	$\langle B_z \rangle_{\rm all}$ [G]	$\langle B_z \rangle_{\rm hydr}$ [G]	Comm.
PDS 2	54610.399	1790	**103±29**	−4±70	ND
47839	54609.968	3375	134±52	141±62	
95881	54609.993	3745	47±25	24±20	
97048	54609.137	2980	**164±42**	**188±47**	ND
97300	54609.047	2495	109±50	96±53	
100453	54610.022	3820	1±14	−30±28	
100546	54610.046	4195	**89±26**	**87±28**	ND
101412	54609.190	3280	**−312±32**	**−454±42**	CD
	54610.081	3525	**−207±28**	**−317±35**	CD
135344B	54609.243	4020	32±15	41±30	
	54610.145	3970	**−38±11**	**−37±12**	ND
139614	54610.201	4010	−40±25	−58±32	
144432	54609.383	2595	36±22	32±42	
144668	54610.238	3710	**−62±18**	**−92±27**	CD
150193	54609.092	3300	**−144±32**	**−252±48**	ND
152404	54609.275	2815	−107±37	−53±23	
158643	54609.275	4165	32±20	14±23	
163296	54610.255	3535	40±30	105±40	
169142	54610.175	3875	50±25	23±32	
VV Ser	54610.332	1050	200±75	376±141	
176386	54610.272	3230	**−119±33**	**−121±35**	ND
179218	54609.360	3855	51±30	28±34	
190073	54609.410	3900	**104±19**	**120±30**	CD
Stars with debris disks					
9672	54345.389	4365	50±22	42±32	
39060	53455.193	4205	−16±14	−36±22	
109573	54610.438	3815	56±30	41±32	
164249	54610.301	2970	19±14	1±25	
172555	54610.287	3875	−35±20	−31±28	
181327	54610.364	3495	−38±16	−75±26	
Standard Ap star with a weak magnetic field					
162725	54549.413	2435	**128±30**	**158±38**	

Notes: All quoted errors are 1σ uncertainties. In Col. 6 we identify new detections by ND and confirmed detections by CD. We note that all claimed detections have a significance of at least 3σ, determined from the formal uncertainties we derive. These measurements are indicated in bold face.

tections of magnetic fields in these stars during this observing run can probably be explained by the strong dependence of the longitudinal magnetic field on the rotational aspect, i.e. on the rotation phase. For the Herbig Ae star HD 163296, we found no indication for the presence of a photospheric magnetic field, in agreement with our previous studies (Hubrig et al. 2006b; Hubrig et al. 2007b).

No definite detection at a significance level of 3σ was achieved for any of the stars with debris disks. The only measurement close to the 3σ level was obtained for the F5/F6V star HD 181327, which belongs to the (∼12 Myr old) β Pictoris moving group, with a measured magnetic field $\langle B_{\rm z} \rangle = -75 \pm 26$ G.

The star HD 101412, with the largest magnetic field strength measured in our sample stars, shows a change of the field strength by ∼100 G during two consecutive nights. In Fig. 2 we present distinct Zeeman features detected at the positions of the hydrogen Balmer lines and the Ca II H&K lines. The Hβ line in the Stokes I spectrum is contaminated by the presence of a variable emission in the line core and was not included in our measurements.

Similar Zeeman features at the positions of the Ca II H&K lines were detected in four other Herbig Ae/Be stars, HD 139614, HD 144668, HD 152404, and HD 190073. In Fig. 3, we present the Stokes V spectra for these stars in the region around the Ca II doublet, together with our previous observation of HD 190073, obtained with FORS 1 in 2005. As we already reported in our earlier studies (Hubrig et al. 2004b, 2006b, 2007b) these lines are very likely formed at the base of the stellar wind, as well as in the accretion gaseous flow, and frequently display multi-component complex structures in both the Stokes V and Stokes I spectra. In two Herbig Ae/Be stars, HD 31648 and HD 190073, such a structure was especially noticeable, and from their study we concluded that a magnetic field is present in both stars, but is most likely of circumstellar origin. For HD 31648, we detected a magnetic field $\langle B_{\rm z} \rangle = 87 \pm 22$ G. Using only the Ca II H&K lines for the measurement of circular polarization in HD 190073, we diagnosed a longitudinal magnetic field at a 2.8σ level, $\langle B_{\rm z} \rangle = 84 \pm 30$ G. Our previous magnetic field measurement for HD 190073 of the order of 80 G was in full agreement with the high resolution spectropolarimetric measurements obtained for this star with ESPaDOnS (Catala et al. 2007), who measured a longitudinal magnetic field $\langle B_{\rm z} \rangle = 74 \pm 10$ G using metal lines. The authors report that they could not see a Stokes V signal in the Ca II H&K lines, but the S/N ratio of their spectra is too low in that spectral region, resulting in a noise level of the order

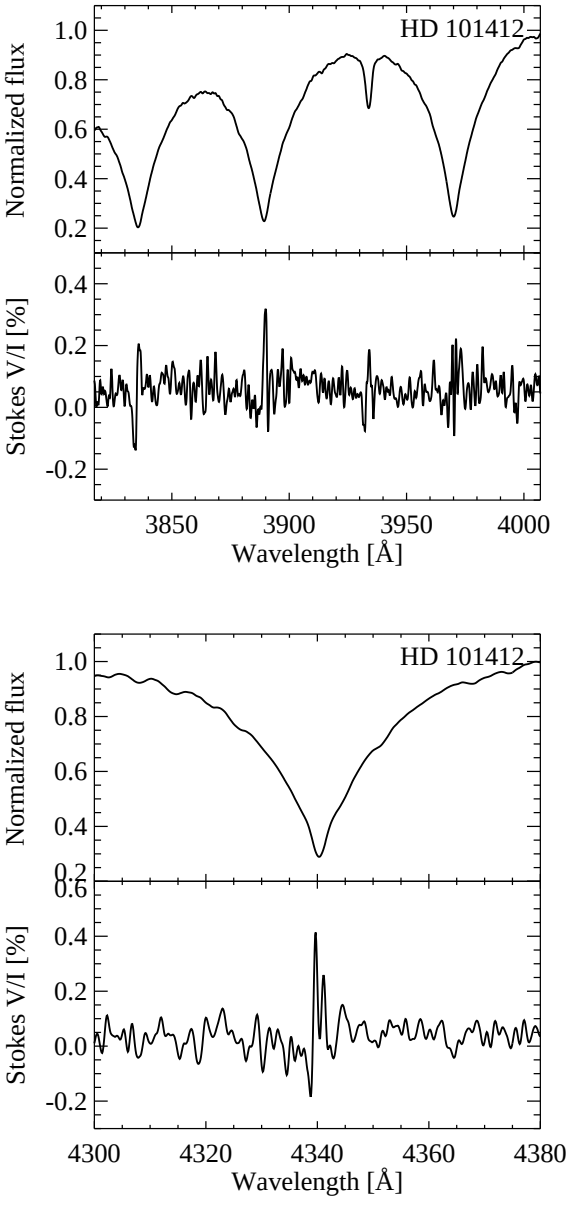

Fig. 2. Stokes I and V spectra of the Herbig Ae/Be star HD 101412, with the largest detected magnetic field. Upper panel: Zeeman features in H_9, H_8, Ca II H&K, and Hϵ profiles. Lower panel: Stokes I and V spectra in the vicinity of the Hγ line.

of 7×10^{-3} in Stokes V per spectral bin of 0.0025 nm, which would not allow them to detect as weak a signal as seen in the LSD average, nor the level of signal reported by Hubrig et al. (2006b). Our new observations reveal a rather large change (by ∼0.5% of circular polarization) in the amplitude of the Zeeman features in the Ca II H&K lines compared to our observations from May 2005 (see the two upper spectra in Fig. 3), indicating a conspicuous variability of the magnetic field.

Wade et al. (2007) mentioned the absence of Zeeman features in the Ca II H&K lines in their FORS 1 spectra of the Herbig stars HD 31648, HD 144432, and HD 144668. On the other hand, in the same study, they report that

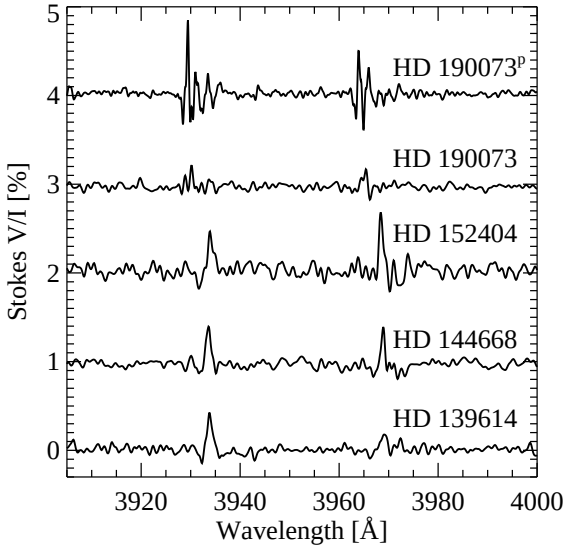

Fig. 3. Stokes V spectra in the vicinity of the Ca II H&K lines of the Herbig Ae/Be stars HD 139614, HD 144668, HD 152404, and HD 190073. At the top we present our previous observation of HD 190073, obtained in May 2005. The amplitude of the Zeeman features in the Ca II H&K lines observed in our recent measurement has decreased by ∼0.5% compared to the previous observations.

their measurements were obtained using a variety of slit widths: 38 of 73 stars were measured with slit widths of 0.″8 to 1″, and 35 of their 73 stars were measured with a slit width of 0.″5. Using wide slits greatly degrades the resolution of the Stokes V spectra, possibly affecting the deduced longitudinal magnetic fields. Wade et al. (2007) looked for this effect in their study, generally not finding strong evidence for it.

4. Discussion of individual stars with magnetic field detections

In the following we discuss the present knowledge of the various observed properties of stars with a magnetic field detection at a 3σ level, placing greater emphasis on the discussion of stars with stronger magnetic fields. Since a few stars of our sample have been previously observed by Wade et al. (2007), we also compare our results with the results obtained by these authors.

4.1. Herbig Ae/Be stars with detected magnetic fields

PDS 2: This star was observed with FORS 1 in November 2004 by Wade et al. (2007). A weak magnetic field of the order of 130–140 G was measured at a 3σ significance level using metal lines and the full spectrum, but could not be diagnosed from the measurements using hydrogen Balmer lines. We achieve a rather similar result: We detect a positive magnetic field $\langle B_z\rangle = 103\pm29$ G using the full spectrum, but we are not able to detect the presence of a magnetic field using hydrogen lines. For this star, no spatially

resolved observations of circumstellar matter or infrared spectral emission features were reported in the literature.

HD 97048: No detection at a 3σ level was achieved by Wade et al. (2007). However, in our observations, the magnetic field in this star is rather strong. We measure $\langle B_z \rangle = 161 \pm 42$ G using the full spectrum and $\langle B_z \rangle = 188 \pm 47$ G using hydrogen lines. A large flaring disk with a mean disk inclination of 42.8° was reported by Doucet et al. (2007) from observations with VISIR. No silicate emission band at 10 μm was found in the mid-IR spectra of HD 97048. The disk has been coronographically imaged by Doering et al. (2007), and its inclination angle appears to be closer to i=30° than the i=42.8° reported by Doucet et al. (2007). The disk has a radial surface brightness profile consistent with dust grain growth and settling, rather than a highly flared geometry. No HH knots are visible in the coronographic ACS F606W image presented by Doering et al. (2007). This is consistent with the at best low level of Mg II emission in the archival IUE data. No presence of a binary companion was detected in the study of Corporon & Lagrange (1999). The mid-IR spectrum is dominated by PAH emission, which arises mostly from an outer radius at 200–300 AU (van Boekel et al. 2004). Both quiescent H_2 emission in the near-IR (Bary et al. 2008) and rotational H_2 emission of warm gas in the mid-IR (Martin-Zaïdi et al. 2007) were reported. HD 97048 was detected in an *XMM-Newton* survey of Cha I. On basis of the negative results of all searches for binarity, Stelzer et al. (2004) ascribed the X-ray emission to the Herbig star.

HD 100546: In this star we measure $\langle B_z \rangle = 89 \pm 26$ G using the full spectrum and $\langle B_z \rangle = 87 \pm 28$ G using hydrogen lines. No detection at a 3σ level was achieved by Wade et al. (2007). Although no stellar companions have been reported, there seems to be evidence for a giant planet forming at ∼6.5 AU (Acke & van den Ancker 2006). The circumstellar disk was repeatedly resolved at optical, near-IR, mid-IR and mm wavelengths. Augereau et al. (2001) derive a disk inclination of 51±3°, while the values from other authors are consistent within error ranges. There is a circumstellar envelope surrounding the disk (e.g. Grady et al. 2001). Silicate emission and PAHs are seen in 10 μm spectra (e.g. Meeus et al. 2001). Highly excited H_2 gas was reported by Martin-Zaïdi et al. (2008), who estimate that the warm H_2 is located within about 1.5 AU from the star. The star is detected in X-rays (Feigelson et al. 2003; Stelzer et al. 2006) with an L_X typical of Herbig Ae stars. No jet is seen in HST imagery in the optical (Grady et al. 2001; Ardila et al. 2007) or in Lyα (Grady et al. 2005a).

HD 101412: Wade et al. (2007) measured a positive magnetic field of the order of 500 G using hydrogen lines. During the first night we measured $\langle B_z \rangle = -312 \pm 32$ G employing the full spectrum and $\langle B_z \rangle = -454 \pm 42$ G on hydrogen lines. The magnetic field was also detected on the second night: $\langle B_z \rangle = -207 \pm 28$ G using the full spectrum and $\langle B_z \rangle = -317 \pm 35$ G on hydrogen lines. Interestingly, Wade et al. (2007) found a negative magnetic field of the same order when they used metal lines for the measurements. Contrary to their results, our measurements show rather consistent results obtained using the full spectrum, metal lines and hydrogen lines, although the magnetic field from metal lines appears somewhat lower, probably due to CS contamination. From the measurements during the first night, using exclusively metal lines, we obtain $\langle B_z \rangle = -158 \pm 50$ G, and $\langle B_z \rangle = -95 \pm 46$ G for the second night.

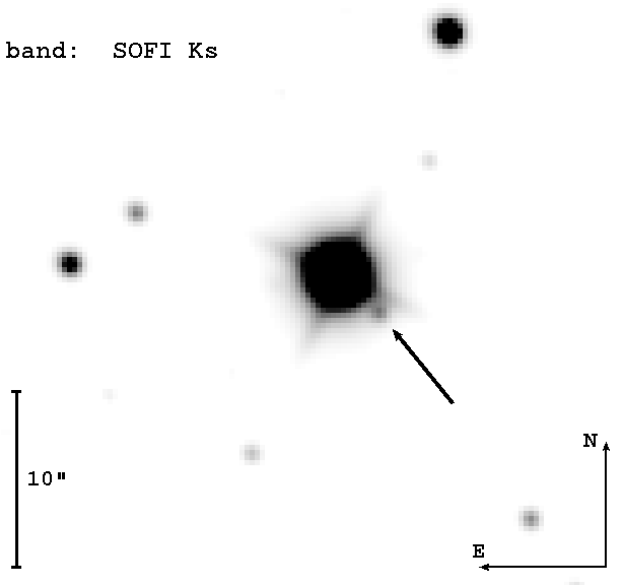

Fig. 4. SOFI Ks-band image of a potential faint companion to HD 101412. The spatial resolution is 0.″29/pix and the separation amounts to 3.″3±0.″2.

It is quite possible that HD 101412 belongs to a visual binary system. In Fig. 4 we present a Ks-band image of HD 101412 obtained with SOFI at the NTT in La Silla. The data were taken in May 2000 in the framework of the ESO programme 65.I-0097(A) and were retrieved from the ESO science data archive. A faint candidate companion is detected at 3.″3±0.″2 separation to the southwest. The spatial resolution of the SOFI images was 0.″29/pix. Whether there is a real physical association between both stars remains to be confirmed.

The very low $v \sin i$=7 km s^{-1} suggests that we may see the disk nearly pole-on. Since this star exhibits the strongest magnetic field and hence is of special interest, we retrieved from the ESO archive three high-resolution UVES spectra of HD 101412 obtained in the framework of ESO programme 077.C-0521(A). An inspection of these spectra, recorded on three different dates, indicates variations in line intensities and line profiles. All lines seem to be variable, and we were not able to find any non-variable spectral line in the spectrum. The largest variations are observed between the dates MJD 53872.540 and MJD 53920.494. A few examples of these variations are presented in Figs. 5 and 6. We tested a number of atmospheric models in the range: $T_{\rm eff}$=8000–11 000 K and $\log g$=4.0–4.5. The studied UVES spectra cover both Hα and Hβ Balmer lines. However, only the wings of the Hβ line can be used to obtain the atmospheric parameters, as the Hα line exhibits strongly variable emission. We obtain as a best fit $T_{\rm eff}$=10 000 K, $\log g$=4.2–4.3 and a $v \sin i$ value of about 5 km s^{-1}. This result is in good agreement with the study of Guimarães et al. (2006) who published $T_{\rm eff}$=10 000±1000 K, $\log g$=4.1±0.4, and $v \sin i$=7±1 km s^{-1}. A good fit is also obtained using the model $T_{\rm eff}$=9000 K and $\log g$=4.0, but the synthetic spectrum for these parameters shows many narrow lines which do not appear in the observed UVES spectra. The

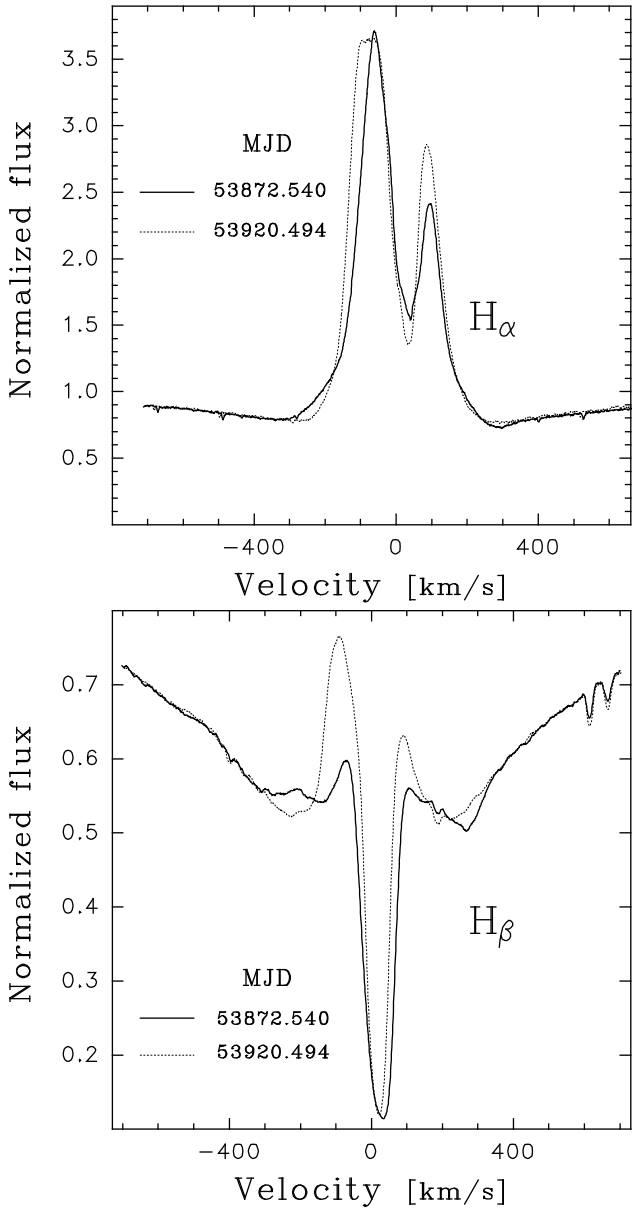

Fig. 5. UVES spectra obtained on two different dates of the Herbig Ae/Be star HD 101412 in the spectral regions around the Hα line (top) and around the Hβ line (bottom).

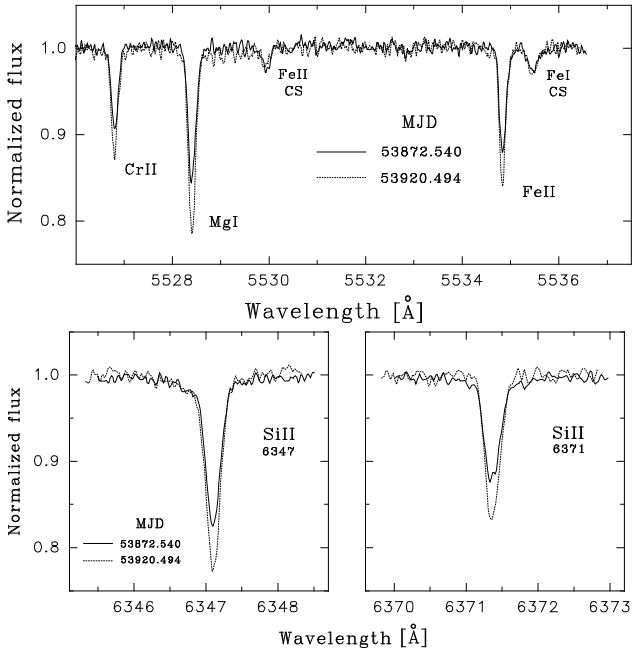

Fig. 6. UVES spectra of the Herbig Ae/Be star HD 101412 in the spectral regions $\lambda\lambda$5526–5538 Å around the Cr II, Mg I, and Fe II lines (upper panel) and around the two Si II lines at λ6347 (lower left panel) and λ6371 (lower right panel). CS lines of Fe I and Fe II are clearly visible in the upper spectrum. Note the strong increase of the line intensities at MJD53920.494.

spectrum is heavily contaminated by CS lines. Two such lines belonging to Fe I and Fe II are clearly visible in Fig. 6.

As we mentioned above, the low $v \sin i$ value suggests that we observe HD 101412 close to pole-on, or that the star is rotating very slowly. The inclination angles of disks of Herbig Ae/Be stars (which are expected to be identical with the inclination angle of the stellar rotation axis) can be reliably derived only for resolved observations of disks. They are usually determined from millimeter observations, coronographic imagery, or near-IR interferometry. On the other hand, the orientation of the disk can be constrained using the emission profile shapes. Type I P Cygni profiles or single emissions all have $i < 40°$. Stars which alternate between type I and type III profiles have $40 < i < 55°$, and stars with double emission all have $i > 55°$. This means that even for objects for which no good disk imagery exists, it is at least possible to constrain their inclination angles from the study of Mg II spectral line profiles in the UV or from the line profile shape of Hα (e.g., Finkenzeller & Mundt 1984; Dunkin et al. 1997). The shape of Hα in the UVES spectra of HD 101412 suggests an inclination angle $i > 55°$, i.e. the star is viewed far from pole-on, in agreement with the recently published value $80° \pm 7°$ by Fedele et al. (2008) who used VLTI/MIDI observations. The slow rotation could in principle be explained by binarity, where the components are synchronized with $P_{\rm rot} = P_{\rm orb}$. However, we detect neither spectral lines of the companion nor any variability of radial velocities in the UVES spectra. It cannot be excluded, though, that braking of the star's rotation is due to its rather strong magnetic field, in analogy with the slow rotation of magnetic Ap and Bp stars. Since the intensities of lines of different elements do not show opposite behaviour, which is usually observed in chemically peculiar Ap and Bp stars, we exclude the presence of chemical spots on the stellar surface. Also the study of temperature sensitive and insensitive lines indicates the absence of temperature spots. Therefore we conclude that the observed spectrum variability has a CS origin. Silicate emission and lower amounts of PAHs are seen in mid-IR spectra (e.g., van Boekel et al. 2005; Geers et al. 2007), while the SED is consistent with a flat disk type (Geers et al. 2007).

HD 135344B=SAO 206462: The detected magnetic field in this star is very weak. We observe a change of the polarity between the first and the second observing night, but the measurement on the first night, using the full spectrum, resulted in a strength of the longitudinal magnetic field $\langle B_{\rm z} \rangle = 32 \pm 15$ G which is only at a 2.1σ significance level. On the second night, the magnetic field was detected

at a 3.2σ level using the full spectrum, $\langle B_z \rangle = -38 \pm 12$ G. As is mentioned in the literature, there has been frequent confusion between HD 135344 and the $\sim 20''$ close, nearby IR source SAO 206462, a mid-F star (Coulson & Walther 1995), also referred to as HD 135344B. Thus SAO 206462 was frequently improperly called HD 135344. A further binary pair was found at $\sim 5\farcs8$ separation from SAO 206462 by Augereau et al. (2001). Mid-IR spectra show silicate absorption around 10 μm (e.g. Acke & van den Ancker 2004) and PAHs (e.g. Sloan et al. 2005). Dent et al. (2005) derived a disk inclination of 11°, obtained from measurements of CO gas. The presence of warm H_2 gas is reported by Thi et al. (2001), which should be treated with caution due to the low S/N and low spatial resolution of ISO data.

This star has recently been identified as the host of a transitional or pre-transitional disk (Brown et al. 2007; Pontoppidan et al. 2008). The disk is coronographically detected at 1.1 μm and 1.6 μm (Grady et al., in preparation) with a radial surface brightness profile consistent with grain growth and settling. No jet is seen in HST optical coronographic imagery (Grady et al. 2005b). FUV excess light and emission were detected by FUSE, with a mass-accretion rate reconcilable with the Brγ measurements (Garcia Lopez 2006; Grady et al., in preparation). The bulk of the FUV emission is consistent with stellar activity, rather than with accretion.

HD 144668=HR 5999: In our previous study (Hubrig et al. 2007a), we showed that the magnetic field of this star is variable, with the strength varying between −75 G and +166 G. Strong Zeeman features are clearly visible at the position of the Ca II H&K lines and hydrogen Balmer lines, similar to those detected in our previous observations (see Fig. 3). We confirm the presence of the magnetic field, measuring $\langle B_z \rangle = -62 \pm 18$ G using the full spectrum and $\langle B_z \rangle = -92 \pm 27$ G using hydrogen lines. In stellar applications, the Stokes V profiles present disk-integrated observations. Generally, stellar magnetic fields are not symmetric relative to the rotation axis, so that the polarization signal changes with the same period as the stellar rotation. The most simple modeling includes a magnetic field approximated by a dipole with an axis inclined to the rotation axis. Recently, Aurière et al. (2007) presented measurements of weak stellar magnetic fields using the cross-correlation technique "Least Squares Deconvolution", originally introduced by Donati et al. (1997). They showed that the presence of a weak magnetic field can be diagnosed from the detection of Stokes V Zeeman signatures, even if the longitudinal magnetic field is very small, as is usually observed during a cross-over phase. In our observations of a few Herbig Ae/Be stars, even at the very low resolution of FORS 1, similar Stokes V Zeeman features are observable in strong Ca II H&K and hydrogen Balmer lines, indicating the presence of a cross-over phase. In Fig. 7 we show an example of Stokes V line profiles of Hγ and Hβ in HD 144668, confirming the presence of a magnetic field in this star at a rotation phase where the longitudinal magnetic field is rather small.

HD 144668 belongs to a quadruple system (Dommanget & Nys 1994), although the orbits and physical relations between the companions are not certain. The nearest neighbour at a separation of $1\farcs4$ appears to be a T Tauri star (Stecklum et al. 1995). A broad but rather shallow 10 μm silicate emission feature indicates grain growth (van Boekel et al. 2005). Preibisch et al. (2006) derived an inclination of 58° from MIDI/VLTI observations and found that the disk

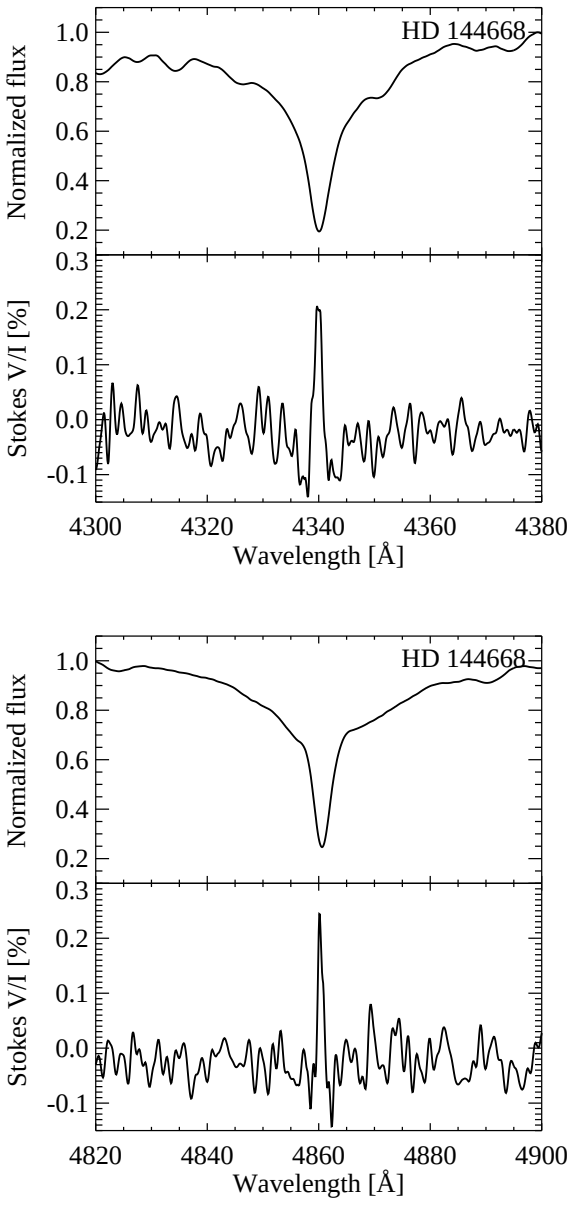

Fig. 7. Stokes I and V spectra of the Herbig Ae/Be star HD 144668. Upper panel: Zeeman feature in the Hγ line. Lower panel: Zeeman feature in the Hβ line.

is very compact with an outer edge of ∼2.6 AU, potentially caused by a further, even closer, yet undetected companion. Recently, HD 144668 was for the first time resolved from its T Tauri companion in X-rays (Stelzer et al. 2009). This observation showed that the bulk of the X-ray emission comes from the companion, but a weak source is associated with HD 144668 (or the hypothesized sub-arcsecond companion).

HD 150193: No attempt had been made to measure the magnetic field in this object. The detected magnetic field is comparatively strong: we measure $\langle B_z \rangle = -144 \pm 32$ G using the full spectrum and $\langle B_z \rangle = -252 \pm 48$ G using hydrogen lines. A binary companion at $1\farcs1$ distance (Reipurth & Zinnecker 1993) is a T Tauri star (e.g. Carmona et al. 2007). Fukagawa et al. (2003) resolved the circumstellar disk in the near-IR and derived a disk inclination of 38±9°.

Broad 10 μm silicate emission is seen in mid-IR spectra (e.g. Acke & van den Ancker 2004). Warm H_2 gas is reported by Thi et al. (2001). Similar to the case of HD 144668, resolved *Chandra* images show that most of the X-ray emission comes from the T Tauri companion, but weak emission is attributed to the Herbig star (Stelzer et al. 2006).

HD 176386: A magnetic field is definitely present: we measure $\langle B_z \rangle = -119 \pm 33$ G using the full spectrum and $\langle B_z \rangle = -121 \pm 35$ G using hydrogen lines. This star is part of a triple system (Dommanget & Nys 1994). Grady et al. (1993) reported evidence for accretion of circumstellar gas onto the star. Martin-Zaïdi et al. (2008) detected warm H_2 gas. This source shows the highest H_2 column density in their entire sample. Both IR (Siebenmorgen et al. 2000) and far-UV spectroscopy (Martin-Zaïdi et al. 2008) suggest that the circumstellar matter has the form of an envelope rather than the form of a disk. PAHs are detected in mid-IR spectra (e.g. Siebenmorgen et al. 2000). Surprisingly, HD 176386 is one of the few Herbig Ae/Be stars confirmed to be X-ray dark ($\log L_X$[erg/s] < 28.6). Stelzer et al. (2006) showed on basis of *Chandra* imaging that apparent X-ray detections of this star in previous lower-resolution observations are to be attributed to the companion at 4″ separation.

HD 190073: A magnetic field of $\langle B_z \rangle = 74 \pm 10$ G was detected using photospheric metal lines with ESPaDOnS (Catala et al. 2007). Our old measurements (Hubrig et al. 2006a) revealed a magnetic field of the order of 80 G at the 2.8σ level, in full agreement with the high resolution ESPaDOnS spectropolarimetric data, whereas Wade et al. (2007) failed to detect the magnetic field in both previous measurements carried out with FORS 1 in November 2004. Our new measurements $\langle B_z \rangle = 104 \pm 19$ G using the full spectrum and $\langle B_z \rangle = 120 \pm 32$ G using hydrogen lines confirm the results presented by Catala et al. (2007). Baines et al. (2006) reported the presence of a potential companion. Silicates and PAHs are seen in the mid-IR (e.g. Boersma et al. 2008). Eisner et al. (2004) showed that interferometric visibilities are consistent with a disk close to face-on, although a significant nonzero inclination cannot be ruled out.

4.2. Stars with measurements suggestive of the presence of magnetic fields

HD 47839=15 Mon: This is a massive O star classified as a pre-main sequence star in SIMBAD. According to Kaper (1996) and Walborn (2006) it shows distinct peculiarities in the spectra, which could be typical for stars possessing magnetic fields. The measured magnetic field is of positive polarity at a 2.6σ significance level, using the full spectrum. The star should be considered as an important target for follow-up studies of magnetic fields in massive stars.

HD 97300: Even though the measured field is only at the $\sim$2σ level, we detect a few distinct Zeeman features in the Stokes V spectrum, supporting the evidence of a magnetic field. This star is a good candidate for future magnetic field measurements. No quiescent H_2 gas was found (Bary et al. 2008). Siebenmorgen et al. (1998) reported the presence of a large circumstellar elliptical ring of PAH emission with thousands of AU in diameter and an indication for the possible existence of a candidate companion. It was also detected as an X-ray source in *ROSAT* and *Chandra* observations (Hamaguchi et al. 2005; Stelzer et al. 2006)

HD 139614: Our previous measurements of HD 139614 revealed the presence of a weak magnetic field in the range from -116 G to -450 G. (Hubrig et al. 2004b; 2006b; 2007b). The current diagnosis of magnetic fields in this star yielded no detection at a 3σ level, neither in Balmer nor in metal lines, with error bars as low as 25 G. In analogy with our previous detections, the measured magnetic field is of negative polarity and Ca II H&K lines in HD 139614 show distinct Zeeman features. The nearly featureless mid-IR continuum of HD 139614 shows small amounts of silicates, but no PAH (Keller et al. 2008).

HD 144432: For this object we measured in the past a magnetic field in the range from -94 G to -119 G (Hubrig et al. 2004b; 2006b; 2007b). Dent et al. (2005) found CO gas and derived a nearly face-on disk orientation. HD 144432 is a binary with $\sim$1.″4 separation (Dommanget & Nys 1994). Carmona et al. (2007) reported the detection of Hα emission and Li absorption in the K5Ve T Tauri companion. The companion is an X-ray source, and weaker X-ray emission is also detected from the position of the Herbig Ae/Be star (Stelzer et al. 2009). The 10 μm silicate emission band shows rather pristine dust, while the SED points towards a flat disk, as reported by Meeus et al. (2001).

HD 152404=AK Sco: The magnetic field $\langle B_z \rangle = 107 \pm 37$ G is detected at the 2.9σ level using the full spectrum. The Stokes V spectrum exhibits distinct Zeeman features at the position of higher number Balmer lines and of the Ca II H&K lines (see for example Fig. 3). This star is one of the best candidates for future spectropolarimetric observations. The *Chandra* image presents one faint X-ray source associated with HD 152404 (Stelzer et al. 2006). Some authors refer to this target as a T Tauri star, as its spectral type may be at the borderline. The 10 μm silicate emission feature indicates very pristine dust (e.g. Przygodda et al. 2003).

VV Ser: The magnetic field is diagnosed only at a significance level of 2.7σ, but additional measurements are desirable. Alonso-Albi et al. (2008) carried out observations at millimeter and centimeter wavelengths towards VV Ser using the Plateau de Bure Interferometer and the Very Large Array to compute the SED from the near infrared to centimeter wavelengths. The modeling of the full SED has provided insights into the dust properties and a more accurate value for the disk mass. The mass of dust in the disk around VV Ser was found to be about 4×10^{-5} $M_\odot$, i.e. 400 times larger than previous estimates. Due to the faintness of the star (m_V=11.6), only two series of two subexposures were taken, each one with an exposure time of 15 min. Pontoppidan et al. (2007b) compared Spitzer infrared data with a disk model and found that the disk is nearly edge-on and self-shadowed by a puffed-up inner disk rim. The 10 μm silicate emission feature is rather weak.

4.3. The observed circumstellar properties of Herbig Ae/Be stars with magnetic field detections discussed in previous studies

HD 31648: Based on interferometric observations, Eisner et al. (2004) determined a disk inclination of $\sim$30° and reported that a binary model can be ruled out with a high degree of confidence. Further, Eisner (2007) found a visibility increase in the Brγ line for this star, as expected for magnetospheric accretion. Piètu et al. (2007) had obtained an inclination angle of $\sim$35° from mm measurements. Silicate

emission was detected in the mid-IR around 10 μm (e.g. Acke & van den Ancker 2004), while the presence of warm H_2 gas is reported by Thi et al. (2001).

HD 104237: This star is at least a quintuple system (Grady et al. 2004), where some components are T Tauri stars. A further spectroscopic companion is suggested by observations of Böhm et al. (2004) and Baines et al. (2006). The Herbig star itself is the brightest X-ray source of the group (Stelzer et al. 2006). The disk is inclined by ∼18° (Grady et al. 2004). Silicate emission is seen in mid-IR spectra (e.g. Acke & van den Ancker 2004). Martin-Zaïdi et al. (2008) found excited and hot H_2 gas from far-UV spectra, while Tatulli et al. (2007) explain the origin of the Brγ emission by an inner disk wind, originating at about 0.5 AU from the star.

HD 200775: This object has a companion detected at 2.″25 (Pirzkal et al. 1997), while spectroscopic observations suggested further binarity of the main component (e.g. Miroshnichenko et al. 1998), which was repeatedly discussed in the literature and later confirmed by Monnier et al. (2006) using interferometry.

V380 Ori: This source is actually a triple system with separations of 3.″0 and 5.″0 (Dommanget & Nys 1994), while the primary itself has a companion at 0.″15 (Leinert et al. 1997) which is probably another Herbig Ae/Be star. Even the superior spatial resolution of *Chandra* is not able to resolve this binary, such that the origin of the X-ray source remains obscure (Stelzer et al. 2006). The broad but shallow 10 μm silicate feature indicates grain growth, as confirmed by van Boekel et al. (2005).

BF Ori: As Mora et al. (2004) showed, the spectra exhibit circumstellar line absorptions with remarkable variations in their strength and dynamical properties. High velocity gas is observed simultaneously in the Balmer and metallic lines and the gaseous circumstellar environment of this star is very complex and active. Silicate emission is detected in 10 μm spectra (e.g. Acke & van den Ancker 2004).

5. Searching for a link between the presence of a magnetic field and fundamental stellar characteristics

Vink et al. (2002) presented their results of Hα spectropolarimetric observations of a sample of 23 Herbig Ae/Be stars, pointing out the possibility of the existence of a physical transition region in the H-R diagram from magnetospheric accretion, similar to that of cTTS, at spectral type A to disk accretion at spectral type B. The main difference between these scenarios is that in the former case the stellar magnetic field truncates the accretion disk at a few stellar radii and gas accretes along magnetic channels from the protoplanetary disk to the star, while in the latter case the accretion flow is not disrupted by the field. Our sample consists of 21 Herbig Ae/Be stars of spectral classification B9 and later spectral types and six debris disk stars. Since the observations of the disk properties of intermediate mass Herbig stars suggest a close parallel to cTTS, it is quite possible that magnetic fields play a crucial role in controlling accretion onto and winds from Herbig Ae stars, similar to the case of the lower-mass cTTS. Evidence for disk accretion in Herbig stars from optical emission line profiles was presented by Muzerolle et al. (2004). However, contrary to the advances achieved in magnetic studies of cTTS, there is still no substantial observational evidence demonstrating the strength, extent, and geometry of magnetic fields in Herbig Ae stars. We are aware of the fact that our observations do not present a systematic monitoring of the magnetic fields of Herbig stars over the rotation period and are just snapshot observations of $\langle B_z \rangle$ values over two visitor nights. However, the magnetic field measurements in these stars are rare due to the very small number of spectropolarimetric facilities on large telescopes, and presently no other magnetic field data are available. Still, as we show in the next sub-sections, a few hints and trends can be established with the obtained data. The search for a link with other stellar properties is important to put preliminary constraints on the mechanism responsible for magnetospheric activity. As we show in the next sub-sections, we establish for the first time preliminary trends.

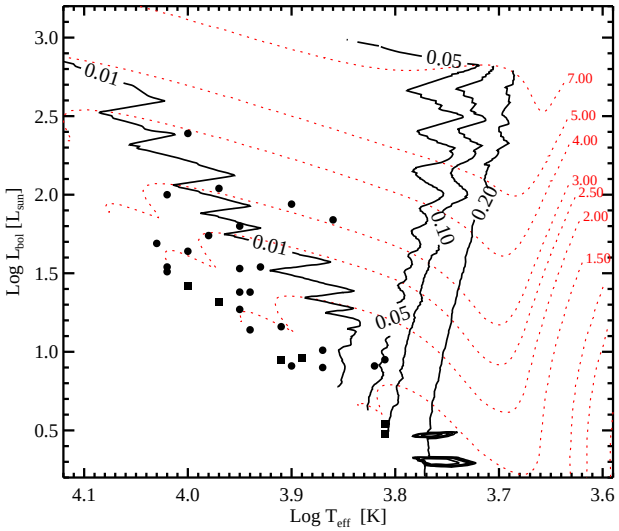

Fig. 8. H-R diagram for all Herbig Ae (filled circles) and debris disk (filled squares) stars from Table 2 on the pre-main sequence models from Siess et al. (2000). Dotted curves show isomass evolutionary tracks and solid jagged contours indicate the size of the convective envelopes labeled in units of the stellar radius.

The H-R diagram for all Herbig Ae and debris disk stars from Table 2 is shown in Fig. 8. In the following, we study the disk properties, binarity, age, and X-ray emission for the Herbig Ae stars and debris disk stars. We include in the definition of 'Herbig Ae' stars targets with spectral type B9 to mid-F. We have estimated the individual stellar masses from an interpolation of the evolutionary tracks from Siess et al. (2000), and list the derived values in Col. 8 of Table 2. As can be seen from Fig. 8, the bulk of our sample has masses between $2-3\,M_{\odot}$. A comparison with evolutionary calculations shows that the majority of the stars in our sample can be considered fully radiative: the depth of the convection zone is less than 1 % (cf. contours in Fig. 8).

In the remainder of this section, we discuss our search for dependencies between the magnetic field and other characteristics of our targets. We have examined various pairs of relevant parameters with correlation tests implemented in ASURV (Astronomy Survival Analysis Package; Lavalley

Table 4. Results from statistical analysis of parameter pairs.

Param 1	Param 2	N	$\tau_{\rm Kend}$	$\rho_{\rm Spear}$
$\log \dot{M}_{acc}$	Age	16	0.05	0.08
B_z	$\log \dot{M}_{acc}$	16	0.68	0.57
$\log L_{\rm x}$	Age	19	0.13	0.28
B_z	$\log L_{\rm x}$	19	0.09	0.07
B_z	$\log (L_{\rm x}/L_{\rm bol})$	19	0.14	0.19
B_z	$P_{\rm rot}$	20	0.50	0.42
B_z	Age	27	0.03	0.05

Notes: Parameter pairs are given in Cols. 1 and 2. N is the number of data points, $\tau_{\rm Kend}$ and $\rho_{\rm Spear}$ denote the probability for no correlation according to Kendall's and Spearman's rank order correlation test, i.e. small numbers indicate that a correlation is present.

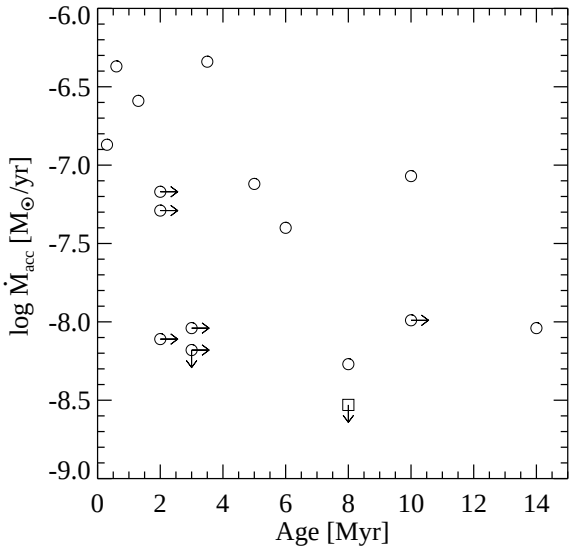

Fig. 9. Mass-accretion rate versus age. Open circles denote Herbig Ae stars and open squares indicate debris disk stars.

et al. 1992). The probabilities for a correlation between two given parameters are summarized in Table 4.

5.1. Accretion rate

The recent results of low resolution linear spectropolarimetric observations of Herbig stars in Hα, Hβ, and Hγ by Mottram et al. (2007) support the presence of magnetospheric accretion in Herbig Ae stars. The authors detected intrinsic line-polarization signatures suggesting that the magnetic accretion scenario generally considered for cTTS may be extended to Herbig Ae stars, but that it may not be extended to early Herbig Be stars, for which the available data are consistent with disk accretion.

The number of Herbig Ae stars with measured mass-accretion rates is still rather low (see Col. 3 in Table 2). In Fig. 9, we show the dependence of mass-accretion rate on age for the stars in our sample. Obviously, the highest mass-accretion rates tend to be found in younger stars.

Table 5. Longitudinal magnetic fields of four previously studied Herbig Ae stars with detections at the 3σ significance level.

Object name	$\langle B_z \rangle_{\rm all}$ [G]
HD 139614	−93±14
HD 144432	−111±16
V380 Ori	460±70
BF Ori	−144±21

In the following figures we use for each studied Herbig star the maximum measured value of the longitudinal field measured from hydrogen lines without taking into account the polarity of the field. In addition, we increased the sample of magnetic Herbig Ae stars by adding to our sample four stars with previous detections of photospheric magnetic fields, namely HD 139614, HD 144432, V380 Ori, and BF Ori. As mentioned in Sect. 1, our previous observations of HD 139614 and HD 144432 revealed the presence of a photospheric magnetic field of the order of ∼100 G (Hubrig et al. 2007b). The longitudinal magnetic field strengths of HD 139614, HD 144432, V380 Ori, and BF Ori are listed in Table 5.

The values of $\dot{M}_{\rm acc}$ were derived by Garcia Lopez et al. (2006) from the measured luminosity of the Brγ emission line, using the correlation between L(Brγ) and the accretion luminosity $L_{\rm acc}$, established by Muzerolle et al. (1998) and Calvet et al. (2004). The correlation used is empirical, which makes no assumptions on the origin of Brγ. An important result found recently by Kraus et al. (2008) is that the Brγ line can trace both mass infall and outflow, implying that Brγ is probably only an indirect tracer of the mass-accretion rate. The authors used the VLTI/AMBER instrument to spatially and spectrally resolve the inner (<5 AU) environment of five Herbig Ae/Be stars (HD 163296, HD 104237, HD 98922, MWC 297, and V921 Sco) in the Brγ emission line as well as in the adjacent continuum. The quantitative analysis for HD 98922 reveals that the line-emitting region is compact enough to be consistent with the magnetospheric accretion scenario, and for the stars HD 163296, HD 104237, MWC 297, and V921 Sco the authors identify an extended stellar wind or a disk wind as the most likely line-emitting mechanism. We have not yet searched for a magnetic field in the star HD 98922, but we observed the star HD 163296 twice. Both observations were non-detections, supporting the results of Kraus et al. (2008) that the magnetospheric accretion scenario does not work for this star. No significant magnetic field detection was achieved for HD 104237 by other authors (e.g. Wade et al. 2007). In Fig. 10, we show the correlation between mass accretion rate and measured longitudinal magnetic fields for our Herbig Ae sample. While we do not see a simple correlation between the magnetic field strength and the mass accretion rate in the data, the observed values are in the range of predictions from magnetospheric accretion models.

Magnetospheric accretion models describe the interaction between a dipolar stellar magnetic field and a surrounding accretion disk assuming pressure equilibrium. The analytical approach yields equations that relate the magnetic field strength to the system parameters (mass, radius, accretion rate, and rotation period; see e.g., Koenigl 1991; Shu et al. 1994). Johns-Krull (2007) has shown that for

the case of cTTS, the models developed by different investigators make consistent predictions on the magnetic field strength.

We examine the magnetospheric accretion scenario for our sample of Herbig Ae stars using the expression for the surface equilibrium field given by Koenigl (1991). We present this relation in the form adopted by Johns-Krull et al. (1999):

$$B_{\rm eq}\,[{\rm kG}] = 3.43 \cdot \left(\tfrac{\epsilon}{0.35}\right)^{7/6} \cdot \left(\tfrac{\beta}{0.5}\right)^{-7/4} \cdot \left(\tfrac{M_*}{M_\odot}\right)^{5/6} \cdot \left(\tfrac{\dot{M}}{10^{-7} M_\odot/{\rm yr}}\right)^{1/2} \cdot \left(\tfrac{R_*}{R_\odot}\right)^{-3} \cdot \left(\tfrac{P_*}{\rm d}\right)^{7/6} \quad (5)$$

where $B_{\rm eq}$ denotes the strength of the equatorial magnetic field in kG, the parameter ϵ expresses the stellar rotation rate in terms of rotation at the inner boundary of a truncated accretion disk, the parameter β describes how effectively the stellar magnetic field couples to the inner regions of the disk, M_* denotes the stellar mass in solar masses, $\dot{M}$ the accretion rate in 10^{-7} solar masses per year, R_* the stellar radius in solar radii, and P_* the stellar rotation period in days.

In Fig. 10, the dotted line represents the prediction from Eq. 5 for a canonical star with $M_* = 2.5\,{\rm M}_\odot$, $R_* = 2.5\,{\rm R}_\odot$, and $P_* = 0.5\,{\rm d}$. We find that the observed field strengths qualitatively support the magnetospheric accretion model for Herbig Ae stars, although the correlation analysis does not yield a positive result for $\langle B_{\rm z}\rangle$ vs. $\dot{M}_{\rm acc}$ (Table 4).

It must be kept in mind that Eq. 5 refers to the equatorial dipole field, while our measured values represent an average of the longitudinal component over the stellar surface and they also depend on the viewing angle.

Future studies of the magnetic field topology and an improvement of indicators of mass-accretion rates are important to understand the role of magnetic fields in the dynamics of the accretion processes in Herbig Ae stars.

5.2. X-ray emission

In Fig. 8 it is demonstrated that our targets have very shallow or completely absent convection zones. Standard dynamo theory does not predict magnetic field generation for fully radiative stars. Our targets are also not hot enough to drive strong radiative winds. Therefore, any X-ray activity is expected to decay with the dissipation of the primordial field. Nevertheless, many Herbig Ae/Be stars are known to be X-ray sources (Zinnecker & Preibisch 1994; Hamaguchi et al. 2005; Stelzer et al. 2006, 2009, and references therein). In the absence of a theoretical model for X-ray production in intermediate-mass stars, the detections have often been ascribed to known or assumed late-type T Tauri star companions. However, recent *Chandra* imaging studies have resolved Herbig Ae/Be stars from most known companions and still came up with very high detection rates (Stelzer et al. 2006, 2009).

We collected X-ray luminosities from the literature, adopting for each star the value from the instrument with the highest spatial resolution available. The $\log L_{\rm X}$ and $\log L_{\rm bol}$ values and the corresponding references are presented in Table 6. Many of the stars of our sample were included in dedicated X-ray imaging studies with *Chandra* aimed at resolving them from their visual late-type companion stars (see references in Table 6). Consequently, only a few of our targets have known unresolved sub-arcsecond or spectroscopic companions that might be responsible for the observed X-ray emission. In particular, AK Sco (=HD 152404) is a spectroscopic binary (Andersen et al. 1989), V380 Ori is both a visual (0.″154) and a spectroscopic binary (Leinert et al. 1997; Corporon & Lagrange 1999), and HR 4796 (=HD 109573) is a 7.″7 binary (Jayawardhana et al. 1998) that could not be resolved with *ROSAT*.

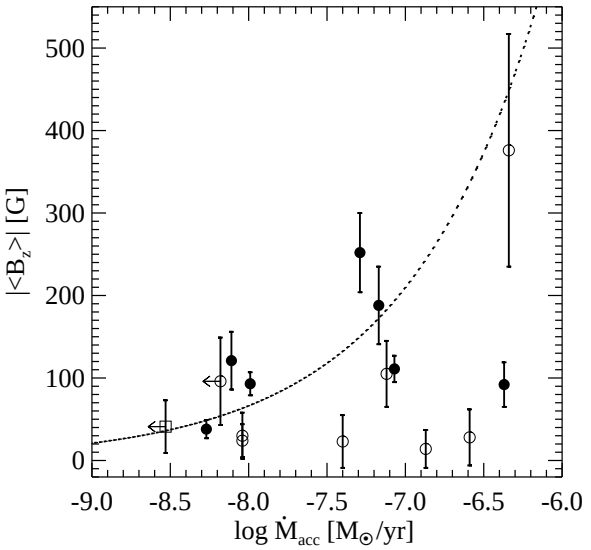

Fig. 10. The strength of the longitudinal magnetic field as a function of accretion rate. Overplotted is the relation predicted by magnetospheric accretion models (see Eq. 5) for assumed stellar parameters of $M_* = 2.5\,{\rm M}_\odot$, $R_* = 2.5\,{\rm R}_\odot$, and $P_* = 0.5\,{\rm d}$. Filled circles denote Herbig Ae stars with a 3σ magnetic field detection, while open circles denote Herbig Ae stars with non-detections. Squares denote stars with debris disks, of which none has a 3σ magnetic field detection.

In Fig. 11 we plot $\log L_{\rm X}$ over the age for our sample stars. It is impossible to exclude categorically that there are further, as yet unknown, companion stars responsible for the X-ray emission. However, given the high detection rate and high spatial resolution of the X-ray studies, this is unlikely to be the case for all stars in this sample.

Tout & Pringle (1995) have suggested a mechanism that can give rise to intrinsic X-ray emission from Herbig Ae/Be stars. In their model, a dynamo can be sustained in a radiative star by rotational shear. As a result of the decrease of the available rotational energy with time, the X-ray luminosity behaves as

$$L_{\rm X} = L_{\rm X,0} \cdot \left(1 + \frac{t}{t_0}\right)^{-3} \quad (6)$$

i.e. it decays from an initial value of $L_{\rm X,0}$ given by the shear energy. Tout & Pringle (1995) showed that an X-ray luminosity of about 1% of the bolometric luminosity can be maintained for a duration of ∼1 Myr, and thereafter decays rapidly according to the law presented in Eq. 6. The curves

Table 6. X-ray emission observed in Herbig Ae stars and debris disk stars.

Object name	log $L_{\rm X}$ [erg/s]	Instrument	log $(L_{\rm X}/L_{\rm bol})$
HD 97048	29.58	*XMM*[a]	−5.64
HD 97300	29.31	*Chandra*[b]	−5.81
HD 100453	28.82	*Chandra*[c]	−5.66
HD 100546	28.93	*Chandra*[b]	−6.16
HD 135344B	∼29.6	*ROSAT*[d]	∼−4.89
HD 144432	28.9	*Chandra*[e]	−5.69
HD 144668	28.3	*Chandra*[e]	−7.22
HD 150193	29.32	*Chandra*[b]	−5.64
HD 152404	29.09	*Chandra*[b]	−5.44
HD 158643	<28.98	*ROSAT*[f]	<−6.99
HD 163296	29.6	*Chandra*[b,g]	−5.36
HD 169142	29.08	*Chandra*[h]	−5.66
HD 176386	<28.56	*Chandra*[b]	<−6.71
HD 39060	26.5	*Chandra*[i]	−8.03
HR 109573	29.4	*ROSAT*[j]	−5.50
HD 172555	<26.9	*Chandra*[k]	<−7.64
HD 181327	<29.4	*ROSAT*[j]	<−4.72
V380 Ori	30.96	*Chandra*[b]	−4.66
BF Ori	<30.2	*ROSAT*[l]	<−4.91

Notes: The log $L_{\rm X}$ values have been collected from the literature, while the log $L_{\rm bol}$ are from Table 2.
References: [a]Stelzer et al. (2004), [b]Stelzer et al. (2006), [c]Collins et al. (2009), [d]Grady et al. ApJ, *submitted*, [e]Stelzer et al. (2009), [f]Berghoefer et al. (1996), [g]Swartz et al. (2005), [h]Grady et al. (2007), [i]Robrade, priv. comm. [j]Stelzer & Neuhäuser (2000), [k]Feigelson et al. (2006), and [l]Hamaguchi et al. (2005).

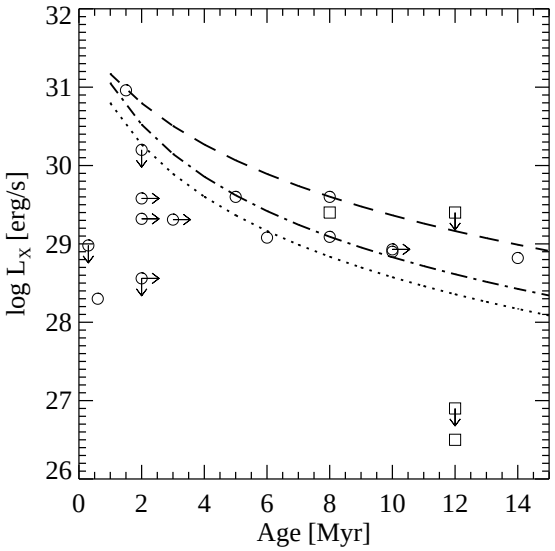

Fig. 11. X-ray luminosity versus age. Symbols are identical to Fig. 9. The decay of $L_{\rm X}$ predicted by the shear dynamo of Tout & Pringle (1995) is shown for different values of the initial parameters t_0 and $L_{\rm X,0}$. The dotted line represents t_0=1 Myr and $L_{\rm X,0}$=5 × 10^{31}, the dashed line represents t_0=2 Myr and $L_{\rm X,0}$=5×10^{31}, and the dash-dotted line t_0=1 Myr and $L_{\rm X,0}$=9 × 10^{31}.

plotted in Fig. 11 represent the predicted decay of the X-ray emission for t_0 = 1 Myr and 2 Myr. The initial X-ray luminosity $L_{\rm X,0}$ was estimated from Eqn. 4.4 of Tout & Pringle (1995) for an assumed M_* = 2.5 $M_\odot$, R_* = 2.5 $M_\odot$, and $L_{\rm bol}$ = 50 $L_\odot$ (dash-dotted line). Two other solutions with a factor of two lower $L_{\rm X,0}$ are also shown.

No clear dependence of the X-ray emission level on the age is noticeable in the data but the absence of stars with high X-ray luminosities at an advanced age is in agreement with the expected decay of the shear dynamo.

In Figs. 12 and 13 we present the strength of the magnetic field plotted versus log $L_{\rm X}$ and log$(L_{\rm X}/L_{\rm bol})$. In both figures we find a hint for an increase of the magnetic field strength with the level of the X-ray emission, also supported by the correlation analysis which yields >90 % probability that a correlation is present between $\langle B_{\rm z}\rangle$ and log $L_{\rm X}$ (Table 4). This could suggest a dynamo mechanism responsible for the coronal activity in Herbig Ae stars. On the other hand, we should keep in mind that the star with the strongest magnetic field in both figures is the spectroscopic binary V380 Ori with $\langle B_{\rm z}\rangle = 460\pm70$ G, and it is not clear yet whether the X-ray emission originates from the primary or from the companion. The filled circle with the lowest strength of the longitudinal magnetic field, $\langle B_{\rm z}\rangle = 37\pm12$ G, belongs in both figures to the Herbig Ae star HD 135344B.

Pevtsov et al. (2003) have derived a universal relation between magnetic flux and X-ray luminosity that holds over 10 orders of magnitudes from the quiet Sun, over solar active regions to active late-type field dwarfs. The unique power-law relation $L_{\rm X} \sim \Psi^{1.13}$ was taken as evidence that the coronae of the Sun and the stars are heated by the same kind of structures. We test whether Herbig Ae stars obey the same relation. The magnetic fluxes of our stars

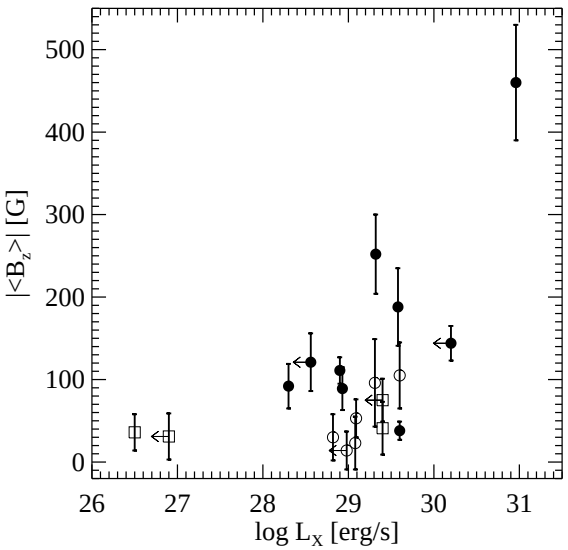

Fig. 12. The strength of the longitudinal magnetic field plotted over the X-ray luminosity. Symbols are identical to Fig. 10.

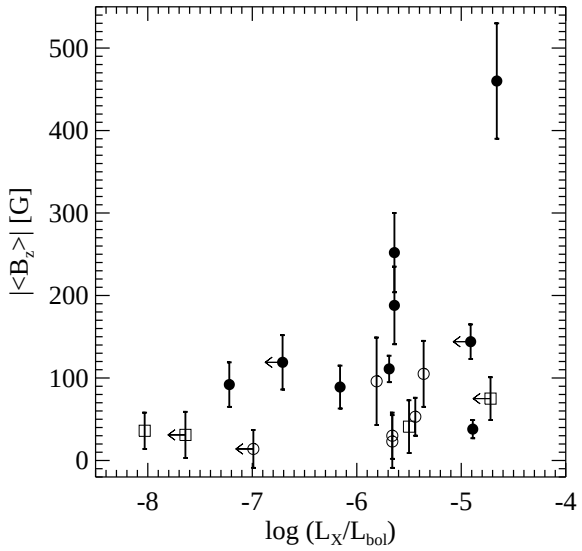

Fig. 13. The strength of the longitudinal magnetic field plotted over the ratio between X-ray luminosity and bolometric luminosity. Symbols are identical to Fig. 10.

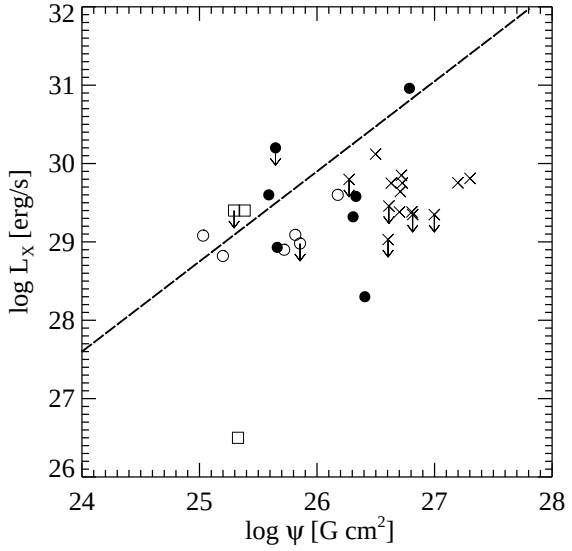

Fig. 14. X-ray luminosity versus magnetic flux for our sample of Herbig Ae stars, and the cTTS sample from Johns-Krull (2007), compared to the power-law relation derived for the Sun and active field stars by Pevtsov et al. (2003). cTTS are represented by crosses. All other symbols are identical to Fig. 10.

are approximated as $\Psi = 12\pi R^2 \overline{\langle B_z \rangle}$, assuming a surface magnetic field $B_s \approx 3\overline{\langle B_z \rangle}$. The magnetic fluxes are plotted in Fig. 14 versus L_X together with the Pevtsov-relation and a sample of cTTS from Johns-Krull (2007). The tendency of the cTTS to show lower than expected X-ray luminosities might be related to the effects of the disk, such as e.g. reduced coronal heating of mass-loaded magnetic field lines (Preibisch et al. 2005) or reduced height of coronal loops (Jardine et al. 2006). Apart from HD 144668 (the lowest filled circle in Fig. 14), the Herbig Ae stars cluster around the line which follows the power law relation derived by Pevtsov. The lowest symbol corresponds to the debris disk star HD 172555.

Clearly, the presence of the X-ray emission in Herbig Ae stars still remains to be explained and more spatially resolved observations are necessary, especially for stars with detected magnetic fields.

5.3. Rotation

Any kind of correlation between the magnetic field strength and the rotation period is of particular importance in view of the unknown origin of magnetic fields in Herbig Ae stars. For example, a trend of the magnetic field strength being lower in more slowly rotating stars would be consistent with the usual prediction for the dynamo theory for stars of a given mass (Mestel 1975). For no Herbig Ae star or debris disk star is the rotation period known. For stars with known disk inclinations and $v \sin i$ values we can estimate $v_{\rm eq}$ values, and from the knowledge of $v_{\rm eq}$ and stellar radius we can estimate the rotation period. The $v \sin i$ values collected from the literature are listed in Col. 4 of Table 7 followed by $v_{\rm eq}$ values in Col. 5. Also most of the radii were collected from the literature. Only for three Herbig Ae stars, HD 101412, HD 135344B, and HD 179218, and two debris disk stars, HD 109573 and HD 181327, have the radii not been estimated in the past. For these stars, we estimated the radii using the Stefan–Boltzmann law. The information on bolometric luminosity and effective temperature of the three Herbig stars was found in van der Plas et al. (2008), while for HD 109573 we used the values presented by Debes et al. (2008) and for HD 181327 we used the values presented by Chen et al. (2006b). Whenever the literature sources permitted, the uncertainties associated with these parameters were included. Using $v_{\rm eq}$ and radii listed in Cols. 5 and 6 of Table 7, respectively, we estimated the rotation periods, which are listed in Col. 7 of Table 7. Magnetic fields are detected in stars with a large range of rotation velocities, from 6 km s^{-1} up to 300 km s^{-1}. No obvious trend of the strength of the longitudinal magnetic field with the rotation velocity or rotation period is identifiable in the statistical tests. The star HD 101412 with the strongest longitudinal magnetic field ($\langle B_z \rangle = 454 \pm 42$ G) clearly stands out in both distributions as it is the most slowly rotating Herbig Ae star, with the longest rotation period of more than 17 days. It is possible that the slow rotation is caused by magnetic braking.

5.4. Age

There are clear indications for a trend towards stronger magnetic fields in younger Herbig Ae stars (Fig. 15), confirmed by statistical tests. The observations of magnetic fields of Herbig Ae stars, their strength and geometry are of a particular importance to understand the origin of magnetic fields in Ap stars. It has been frequently mentioned in the literature that magnetic Herbig Ae stars are potential progenitors of the magnetic Ap stars (e.g., Stepien & Landstreet 2002; Catala 2003; Wade et al. 2005). On

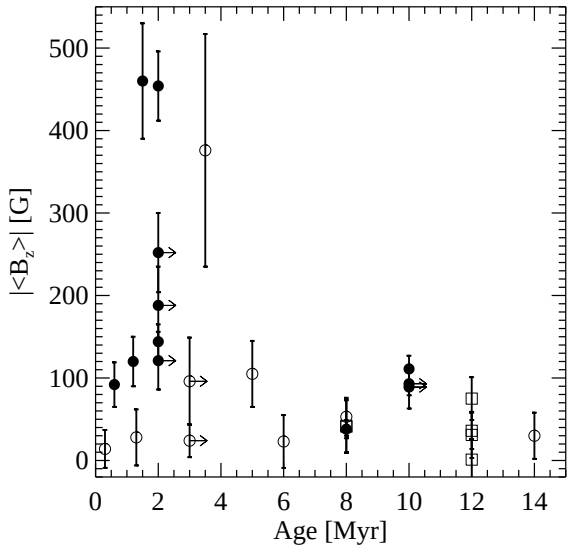

Fig. 15. The strength of the longitudinal magnetic field as a function of age. The symbols are identical to Fig. 10.

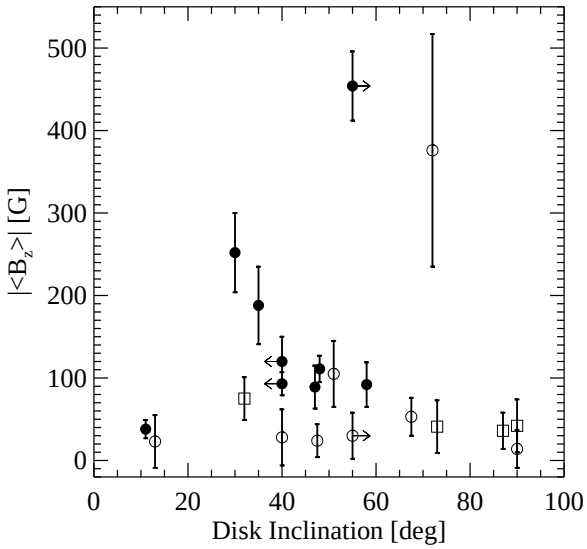

Fig. 16. The strength of the longitudinal magnetic field versus disk inclination angles. Symbols are identical to Fig. 10.

the other hand, from Fig. 15 it is obvious that stronger magnetic fields appear in very young Herbig Ae stars, and the magnetic fields become very weak at the end of their PMS life. These results clearly confirm the conclusions of Hubrig et al. (2000, 2005, 2007a) that magnetic fields in stars with masses less than $3\,M_{\odot}$ are rarely found close to the ZAMS and that kG magnetic fields appear in A stars already evolved from the ZAMS. In contrast, magnetic Bp stars with masses $M{>}3\,M_{\odot}$ seem to be concentrated closer to the ZAMS.

5.5. Disk properties

In the following, we compare the magnetic field and accretion rate to some relevant disk properties.

5.5.1. Disk inclination

Although an expanding sample of Herbig Ae stars have system inclination data from CO and coronographic imaging surveys, for a major part of the studied Herbig Ae stars the orientation of the disk still has to be constrained using line profiles as a proxy for the inclination, as described in Sect. 4. The emission profile shapes of Mg II lines from UV studies or the Hα line profiles are frequently used. We present the inclination angles collected from different papers in the second column of Table 7. Our own estimates of profile types from the study of Mg II spectral line profiles in UV spectra are listed in the comments with running indices close to the HD numbers. In the third column we present the adopted inclinations. Using inclination angles in combination with $v \sin i$ data, we derive $v_{\rm eq}$ (Col. 4 of Table 7).

However, no correlation between mass-accretion rate and disk inclination is detected. We also do not find any trend of the measured longitudinal magnetic field with the inclination angle (Fig. 16).

The disk inclinations for our magnetic Herbig Ae stars sample the whole possible range from close to face-on to close to edge-on. The strongest magnetic fields in our sample are observed for a flared disk (HD 97048), for an edge-on disk (HD 101412) and for close to pole-on disks (HD 150193 and HD 190073), and systems with an envelope rather than a disk (HD 85567 and HD 176386). These results show that there is no preferred disk orientation for the detection of a magnetic field.

5.5.2. Disk geometry

We find that magnetic fields are detected in systems both with and without strong PAHs, but appear to be more frequent in the first, flared case. This result could probably indicate an age dependence of the presence of magnetic fields. Acke et al. (2004) studied Herbig Ae/Be stars with different IR SEDs with the conclusion that flaring disks probably evolve into self-shadowed disks. The existence of strong PAH emission may point to a flared disk, since the PAH grains reside further outside in the disk, whereas they would be destroyed near the hot inner disk rim. On the other hand, Keller et al. (2008) conclude that most Herbig Ae/Be stars have PAH emission at some level, and there is no correlation of PAH emission with the disk geometry. Since PAHs originate from the inner 200–300 AU of the disk, they are actually not a good measure of magnetic properties of the Herbig stars. Silicates usually emerge from ∼1 AU and beyond. Contrary to the silicates, the PAHs need to be excited by direct stellar irradiation, which may not work well in a flat disk. In addition, the IR slope of the SED can further indicate whether the disk is flat or flared (Meeus et al. 2001). We note that magnetic fields are also detected in HD 176386.

Table 7. Rotation periods of stars with known inclinations.

Object name	Inclination Measurements [°]	Adopted Inclination [°]	$v \sin i$ [km s^{-1}]	$v_{\rm eq}$ [km s^{-1}]	R [$R_\odot$]	P [d]
HD 95881	40−55[1]	40−55	50[q]	61−78	3.1[dd]	2.0−2.6
HD 97048	30−40[a]	30−40	140[r]	218−280	2.5[ee]	0.5−0.6
	42.8[b]					
HD 100453	>55[2]	>55	39[s]	<48	1.7[ff]	>1.8
HD 100546	42[c]	47±5	65[t]	82−97	1.7[ff]	0.9−1.0
	51[d]					
HD 101412	>55[3]	>55	5[u]	<6.1	2.1[gg]	>17.4
HD 135344B	11[e]	11	69[v]	362	2.4[gg]	0.3
	14[f]					
HD 139614	<40[g]	<40	15[w]	>23	1.6[dd]	<3.5
HD 144432	48±10[e]	48±10	70[w]	83−114	3.0[ff]	1.3−1.8
HD 144668	58[h]	58	100[w]	118	3.9[ee]	1.7
HD 150193	∼38[i]	30[5]	100[t]	200	2.1[ee]	0.5
HD 152404	65−70[j]	65−70	18.5±1[j]	18.5−21.5	2.6[dd]	6.1−7.1
HD 158643	∼90[k]	90	267±5[v]	267±5	5.3[hh]	1.0
			228[x]	228		
HD 163296	$51^{+11,l}_{-9}$	51	130[w]	167	2.8[ee]	0.8
HD 169142	13±2[e]	13±2	66±2[v]	247−356	1.6[dd]	0.2−0.3
VV Ser	72±5[f]	72	142[y]	149	2.4[ee]	0.8
			229[z]	241		
HD 179218	40±10[e]	40±10	60[aa]	78−120	4.8[gg]	2.0−3.1
HD 190073	<40[4]	<40	12[bb]	>18.7	3.3[ff]	<8.9
HD 9672	90[m]	90	196[x]	196	1.7[ii]	0.4
HD 39060	87[n]	87	130[k]	130	1.8[jj]	0.7
HD 109573	73[o]	73	152[x]	159	1.8[gg]	0.6
HD 181327	31.7[p]	31.7	16[cc]	30	1.2[gg]	2.0

Notes: Inclination angles derived for resolved disk detections from the literature and from the study of Mg II spectral line profiles in UV spectra or the study of Hα line profiles in optical spectra and the inclination values we finally adopt for further use are listed in Cols. 2 and 3. $v \sin i$ values and radii presented in Cols. 4 and 6, respectively, are for the most part gathered from the literature. In Col. 7 we present the equatorial velocity values which are obtained from the inclination angles and the $v \sin i$ values. $v_{\rm eq}$ and radii are used to estimate the rotation periods listed in the last column. Radii marked as *this study* were calculated using $T_{\rm eff}$ and bolometric luminosity, both taken from the literature.
References: [a]Doering et al. (2007), [b]Doucet et al. (2007), [c]Ardila et al. (2007), [d]Augereau et al. (2001), [e]Dent et al. (2005), [f]Pontoppidan et al. (2008), [g]Meeus et al. 1998, [h]Preibisch et al. (2006), [i]Fukagawa et al. (2003), [j]Alencar et al. (2003), [k]Slettebak (1982), [l]Wassell et al. (2006), [m]Hughes et al. (2008), [n]Heap et al. (2000), [o]Schneider et al. (1999), [p]Schneider et al. (2006), [q]Grady et al. (1996), [r]van den Ancker (1998), [s]Acke & Waelkens (2004), [t]Hamidouche et al. (2008), [u]this study (see Subsect. 4.1), [v]Dunkin et al. (1997), [w]Hubrig et al. (2007b), [x]Royer et al. (2007), [y]Vieira et al. (2003), [z]Mora et al. (2001), [aa]Bernacca & Perinotto (1970), [bb]Pogodin et al. (2005), [cc]de la Reza & Pinzón (2004), [dd]Blondel & Tjin (2006), [ee]Hillenbrand et al. (1992), [ff]Wade et al. (2007), [gg]this study (see table caption), [hh]Tatulli et al. (2008), [ii]Hughes et al. (2008), and [jj]di Folco et al. (2004).
Comments on the inclination angles deduced in this study, mainly from IUE (LWR and LWP cameras) through analysis of line profile types. Profile shapes are classified according to Beals (1951). See also the discussion in Subsect. 4.1. [1]Mg II alternates between P Cygni type I (red emission, with blue-shifted absorption, IUE LWP 30772) and type III (double emission, IUE LWP 13082), [2]the Hα profile shown by Meeus et al. (2002) shows characteristic double-peaked Hα emission, [3]see the discussion in Subsect. 4.1, [4]Mg II has a type I P Cygni profile (IUE LWP 25762, LWR 11977, LWR 08996), [5]Mg II has a type I profile (IUE LWP 13083).

5.5.3. Hot disk gas

For many of our targets with a detected magnetic field, reports on the detection of excited, hot inner disk gas exist, which may be attributed to a gaseous accretion ring close to the star (see especially Tatulli et al. 2007; Isella et al. 2008).

Activity in the inner disk is often accompanied by an increased K-band excess. To prove whether there is a direct trend, we correlated the K-band excess, derived as the difference of the measured and expected K-band flux of each star, with the strength of its magnetic field, but we found no correlation. We compared intrinsic V-K colours, as given e.g. by Koornneef (1983), to the difference V–K in the measured photometry of both passbands, as given in SIMBAD. Due to a missing luminosity class we assumed a class V for PDS 2, HD 97048, VV Ser and HD 179218. We obtained excesses between 0.0 and 3.9 mag, with an uncertainty of 0.1 mag. The lack of correlation may be explained by the fact that without spectral resolution it is not possible to determine if the K-band excess is due to gas lines or to a hot inner dust continuum. A hot inner dust continuum will as well produce an increased broad-band K excess, possibly

without being related to the magnetic field. While there is a clear trend that most of the magnetic Herbig Ae stars have reports on hot, inner gas, a selection effect cannot be ruled out, as many of the non-magnetic Herbig Ae stars may just not have been measured in a similar way.

5.6. Binarity

A majority of the Herbig Ae/Be stars are binary or multiple systems. The existence of a magnetic field, however, does not seem to be related to binarity. We note however, that the presence of a close companion contributing to the observed spectropolarimetric spectra can cause a non-detection of the magnetic field due to blending of spectral lines of the primary. The contribution of the secondary component can be disentangled only by means of high resolution spectropolarimetric observations, but not with low resolution FORS 1 spectropolarimetry. In the present study, some targets, e.g. HD 97048 or HD 100546, show a magnetic field, but have no known companions, while other binary Herbig Ae stars possess no magnetic field.

6. Summary

In the course of our spectropolarimetric study of Herbig Ae/Be stars, we detected magnetic fields in six stars for the first time, PDS 2, HD 97048, HD 100546, HD 135344B, HD 150193, and HD 176386. The presence of a magnetic field was confirmed in the stars HD 101412, HD 144668, and HD 190073.

We have for the first time examined the relation of the measured field strengths to various parameters that characterize the star-disk system.

Among the most important relations for the interpretation of the fields is the one between magnetic field strength and accretion rate. We do not find a clear trend between these two parameters in our sample of Herbig Ae stars but the measured field strengths are compatible, in order of magnitude, with the values expected from magnetospheric accretion scenarios for a dipole field (tens to a few hundreds of Gauss). This contrasts with the situation for cTTS. For typical cTTS parameters, accretion models predict fields that range between ∼200–2000 G. However, the observed mean magnetic field strengths of cTTS are not correlated with the predictions (Johns-Krull 2007). For most cTTS, the observed fields are larger than the expected values, possibly indicating that magnetic field pressure dominates gas pressure in these systems. In addition, the dipole approximation is known not to be valid for the case of cTTS that have complex field geometries (e.g. Gregory et al. 2008), while our results suggest that it may be a reasonable description of Herbig Ae stars.

We find that stronger magnetic fields tend to be found in younger Herbig stars. The magnetic fields become very weak or completely disappear in stars when they arrive on the ZAMS. Similarly, strong X-ray sources are only found at the youngest ages, in qualitative agreement with the predictions of a shear dynamo that decays within a few Myrs as the rotational energy of the star decreases (Tout & Pringle 1995). It is premature, however, to claim a direct connection between magnetic field and X-ray luminosity. The Herbig Ae stars seem to follow the power-law between magnetic flux and X-ray luminosity established for the Sun and main-sequence active stars.

We do not find any trend between the presence of a magnetic field and disk inclination angles. The membership in binary or multiple systems does not seem to have any impact on the presence of a magnetic field, whereas there is a hint that the appearance of magnetic fields is more frequent in Herbig stars with flared disks and hot, inner gas. Since flared disks are the least evolved, this is possibly another indication for the decay of magnetic fields with increasing age. However, no trend of the strength of the magnetic field with rotation velocity and rotation period was detected in our study.

While considerable progress has been made with respect to the presence of magnetic fields in Herbig Ae stars, a number of questions remain open. The most important question is related to the origin of the magnetic fields in these stars. Although our results provide new clues, the observational results presented in this work are still inconclusive as to the magnetic field origin. Tout & Pringle (1995) proposed a non-solar dynamo that could operate in rapidly rotating A-type stars based on rotational shear energy. Their model predicts that the coronal activity at the observed rates of $\log L_X$ can be sustained for a period of the order of 10^6 yr. Other possible mechanisms causing magnetic activity involve fossil magnetic fields or magnetically confined wind shocks (e.g. Babel & Montmerle 1997). A more comprehensive survey of the presence of magnetic fields and a detailed study of the magnetic field topology in a Herbig star sample of increased size will provide important additional information to test the predictions of different theories. About half of the stars with magnetic field detections possess longitudinal magnetic fields larger than 100 G. These stars are the best candidates for future spectropolarimetric studies to analyze the behaviour of their magnetic fields over the rotational periods to disclose the magnetic topology on their surfaces and to study the complex interaction between the stellar magnetic field, the disk and the stellar wind.

Acknowledgements. BS acknowledges financial support from ASI/INAF under contract I/088/06/0, MAP and RVY acknowledge RFBR grant No 07-02-00535a and Sci.Schole No 6110.2008.2, and MC acknowledges DIUV grant 08/2007. This research has made use of the SIMBAD database, operated at CDS, Strasbourg, France.

References

Acke, B., & van den Ancker, M. E. 2004, A&A, 426, 151
Acke, B., & van den Ancker, M. E. 2006, A&A, 449, 267
Acke, B., van den Ancker, M.E., Dullemond, C.P., et al. 2004, A&A, 422, 621
Acke, B., & Waelkens, C. 2004, A&A, 427, 1009
Alecian, E., Catala, C., Wade, G. A., et al. 2008, MNRAS, 385, 391
Alencar, S. H. P., Melo, C. H. F., Dullemond, C. P., et al. 2003, A&A, 409, 1037
Alonso-Albi, T., Fuente, A., Bachiller, R., et al. 2008, ApJ, 680, 1289
Alonso-Albi, T., Fuente, A., Bachiller, R., et al. 2009, A&A, 497, 117
Andersen, J., Lindgren, H., Hazen, M. L., & Mayor, M. 1989, A&A, 219, 142
Ardila, D. R., Golimowski, D. A., Krist, J. E., et al. 2007, ApJ, 665, 512
Augereau, J. C., Lagrange, A. M., Mouillet, D., & Ménard, F. 2001, A&A, 365, 78
Aurière, M., Wade, G. A., Silvester, J., et al. 2007, A&A, 475, 1053
Babel, J., & Montmerle, Th. 1997, A&A, 323, 121
Bagnulo, S., Landstreet, J. D., Mason, E., et al. 2006, A&A, 450, 777
Baines, D., Oudmaijer, R. D., Porter, J. M., & Pozzo, M. 2006, MNRAS, 367, 737
Bary, J. S., Weintraub, D. A., Shukla, S. J., et al. 2008, ApJ, 678, 1088

Beals, C. S. 1951, MNRAS, 111, 202
Berghoefer, T. W., Schmitt, J. H. M. M., & Cassinelli, J. P. 1996, A&AS, 118, 481
Bernacca, P. L., & Perinotto, M. 1970, Contr. Oss. Astrof. Padova in Asiago, 239, 1
Beskrovnaya, N. G., & Pogodin, M. A. 2004, A&A, 414, 955
Blondel, P. F. C., & Tjin A Djie, H. R. E. 2006, A&A, 456, 1045
Boersma, C., Bouwman, J., Lahuis, F., et al. 2008, A&A, 484, 241
Böhm, T., Catala, C., Balona, L., & Carter, B. 2004, A&A, 427, 907
Brown, A., Linsky, J. L., Walter, F., et al. 1985, BAAS, 17, 837
Brown, J. M., Blake, G. A., Dullemond, C. P., et al. 2007, ApJ, 664, L107
Calvet, N., Muzerolle, J., Briceño, C., et al. 2004, ApJ, 128, 1294
Carmona, A., van den Ancker, M. E., & Henning, Th. 2007, A&A, 464, 687
Carpenter, J. M., Mamajek, E. E., Hillenbrand, L. A., & Meyer, M. R. 2006, ApJ, 651, L49
Catala, C. 2003, Ap&SS, 284, 53
Catala, C., Alecian, E., Donati, J.-F., et al. 2007, A&A, 462, 293
Chen, X. P., Henning, T., van Boekel, R., & Grady, C. A. 2006a, A&A, 445, 331
Chen, C. H., Sargent, B. A., Bohac, C., et al. 2006b, ApJS, 166, 351,
Collins, K. A., Grady, C. A., Hamaguchi, K., et al. 2009, ApJ, 697, 557
Corcoran, M., & Ray, T. P. 1998, A&A, 331, 147
Corporon, P., & Lagrange, A.-M. 1999, A&AS, 136, 429
Coulson, I. M., & Walther, D. M. 1995, MNRAS, 274, 977
Debes, J. H., Weinberger, A. J., & Schneider, G. 2008, ApJL, 673, 191
de la Reza, R., & Pinzón, G. 2004, AJ, 128, 1812
Dent, W. R. F., Greaves, J. S., & Coulson, I. M. 2005, MNRAS, 359, 663
Di Folco, E., Thévenin, F., Kervella, P., et al. 2004, A&A, 426, 601
Doering, R. L., Meixner, M., Holfeltz, S. T., et al. 2007, AJ, 133, 2122
Dommanget, J., & Nys, O. 1994, Com. de l'Observ. Royal de Belgique, 115, 1
Donati, J.-F., Semel, M., Carter, B. D., et al. 1997, MNRAS, 291, 658
Doucet, C., Habart, E., Pantin, E., et al. 2007, A&A, 470, 625
Dullemond, C. P., Dominik, C., & Natta, A. 2001, ApJ, 560, 957
Dunkin, S. K., Barlow, M. J., & Ryan, S. G. 1997, MNRAS, 290, 165
Eisner, J. A., Lane, B. F., Hillenbrand, L. A., et al. 2004, ApJ, 613, 1049
Eisner, J. A. 2007, Nature, 447, 562
Fedele, D., van den Ancker, M. E., Acke, B., et al. 2008, A&A, 491, 809
Feigelson, E. D., & Montmerle, T. 1999, ARA&A, 37, 363
Feigelson, E. D., Lawson, W. A., & Garmire, G. P. 2003, ApJ, 599, 1207
Feigelson, E. D., Lawson, W. A., Stark, M., et al. 2006, AJ, 131, 1730
Finkenzeller, U., & Mundt, R. 1984, A&AS, 55, 109
Folsom, C. P., Wade, G. A., Bagnulo, S., & Landstreet, J. D. 2007, MNRAS, 376, 361
Fukagawa, M., Tamura, M., Itoh, Y., et al. 2003, ApJ, 590, L49
Garcia Lopez, R., Natta, A., Testi, L., & Habart, E. 2006, A&A, 459, 837
Geers, V. C., van Dishoeck, E. F., Visser, R., et al. 2007, A&A, 476, 279
Grady, C. A., Perez, M. R., & The, P. S. 1993, A&A, 274, 847
Grady, C. A., Perez, M. R., Talavera, A., et al. 1996, A&AS, 120, 157
Grady, C. A., Polomski, E. F., Henning, Th., et al. 2001, AJ, 122, 3396
Grady, C. A., Woodgate, B., Torres, C. A. O., et al. 2004, ApJ, 608, 809
Grady, C. A., Woodgate, B., Heap, S. R., et al. 2005a, ApJ, 620, 470
Grady, C. A., Woodgate, B E., Bowers, C. W., et al. 2005b, ApJ, 630, 958
Grady, C. A., Schneider, G., Hamaguchi, K., et al. 2007, ApJ, 665, 1391
Gregory, S. G., Matt, S. P., Donati, J.-F., & Jardine, M. 2008, MNRAS, 389, 1839
Guimarães, M. M., Alencar, S. H. P., Corradi, W. J. B., & Vieira, S. L. A. 2006, A&A, 457, 581
Hamaguchi, K., Yamauchi, S., & Koyama, K. 2005, ApJ, 618, 360
Hamidouche, M., Wang, S., & Looney L. W. 2008, AJ, 135, 1474
Hartigan, P., Edwards, S., & Ghandour, L. 1995, ApJ, 452, 736
Heap, S. R., Lindler, D. J., Lanz, Th. M., et al. 2000, ApJ, 539, 435
Herbig, G. H. 1960, ApJS, 4, 337
Hillenbrand, L. A., Strom, S. E., Vrba, F. J., & Keene, J. 1992, ApJ, 397, 613
Hubrig, S., North, P., & Mathys, G. 2000, ApJ, 539, 352
Hubrig, S., Kurtz, D. W., Bagnulo, S., et al. 2004b, A&A, 415, 661
Hubrig, S., Schöller, M., & Yudin, R. V. 2004a, A&A, 428, L1
Hubrig, S., Szeifert, T., Schöller, M., et al. 2004c, A&A, 415, 685
Hubrig, S., Schöller, M., & North, P. 2005, AIPC, 784, 145
Hubrig, S., North, P., Schöller, M., & Mathys, G. 2006b, AN, 327, 289
Hubrig, S., Yudin, R. V., Schöller, M., & Pogodin, M. A. 2006a, A&A, 446, 1089
Hubrig, S., North, P., & Schöller, M. 2007b, AN, 328, 475
Hubrig, S., Pogodin, M. A., Yudin, R. V., et al. 2007a, A&A, 463, 1039
Hughes, A. M., Wilner, D. J., Kamp, I., & Hogerheijde, M. R. 2008, ApJ, 681, 626
Isella, A., Tatulli, E., Natta, A., & Testi, L. 2008, A&A, 483, L13
Jardine, M., Cameron, A. C., Donati, J.-F., et al. 2006, MNRAS, 367, 917
Jayawardhana, R., Fisher, S., Hartmann, L., et al. 1998, ApJ, 503, L79
Johns-Krull, C. M. 2007, ApJ, 664, 975
Johns-Krull, C. M., Valenti, J. A., & Koresko, C. 1999, ApJ, 516, 900
Kamp, I., & Dullemond, C. P. 2004, ApJ, 615, 991
Kaper, L., Henrichs, H. F., Nichols, J. S., et al. 1996, A&AS, 116, 257
Keller, L. D., Sloan, G. C., Forrest, W. J., & Ayala, S. 2008, ApJ, 684, 411
Kessler-Silacci, J. E., Hillenbrand, L. A., Blake, G. A., & Meyer, M. R. 2005, ApJ, 622, 404
Koenigl, A. 1991, ApJL, 370, L39
Koornneef, J. 1983, A&A, 128, 84
Kraus, S., Hofmann, K.-H., Benisty, M., et al. 2008, A&A, 489, 1157
Landstreet, J. D., Silaj, J., Andretta, V., et al. 2008, A&A, 481, 465
Lavalley, M., Isobe, T., & Feigelson, E. 1992, In: "Astronomical Data Analysis Software and Systems I", Eds. D. M. Worrall, C. Biemesderfer, & J. Barnes, Astron. Soc. of the Pacific Conf. Ser., 25, 245
Leinert, C., Richichi, A., & Haas, M. 1997, A&A, 318, 472
Markova, N., Puls, J., Repolust, T., & Markov, H. 2004, A&A, 413, 693
Martin-Zaïdi, C., Lagage, P.-O., Pantin, E., & Habart, E. 2007, ApJ, 666, L117
Martin-Zaïdi, C., Deleuil, M., Le Bourlot, J., et al. 2008, A&A, 484, 225
McKee, C. F., & Ostriker, E. C. 2007, ARA&A, 45, 565
Meeus, G., Waelkens, C., & Malfait, K. 1998, A&A, 329, 131
Meeus, G., Waters, L. B. F. M., Bouwman, J., et al. 2001, A&A, 365, 476
Meeus, G., Bouwman, J., Dominik, C., et al. 2002, A&A, 392, 1039,
Melnikov, S., Woitas, J., Eislöffel, J., et al. 2008, A&A, 483, 199
Mestel, L. 1975, In: "Physics of Ap Stars", Eds. W. W. Weiss, H. Jenkner, & C. Jaschek, IAUC 32, Vienna, Universitätssternwarte, 1
Miroshnichenko, A.S., Mulliss, C.L., Bjorkman, K.S., et al. 2004, PASP, 110, 883
Monnier, J. D., Millan-Gabet, R., Billmeier, R., et al. 2005, ApJ, 624, 832
Monnier, J. D., Berger, J.-P., Millan-Gabet, R., et al. 2006, ApJ, 647, 444
Mora, A., Merín, B., Solano, E., et al. 2001, A&A, 378, 116
Mora, A., Eiroa, C., Natta, A., et al. 2004, A&A, 419, 225
Mottram, J. C., Vink, J. S., Oudmaijer, R. D., & Patel, M. 2007, MNRAS, 377, 1363
Muzerolle, J., D'Alessio, P., Calvet, N., & Hartmann, L. 2004, ApJ, 617, 406
Muzerolle, J., Hartmann, L., & Calvet, N. 1998, AJ, 116, 2965
Muzerolle, J., D'Alessio, P., Calvet, N., & Hartmann, L. 2004, ApJ, 617, 406
Najita, J. 2004, In: "Star Formation in the Interstellar Medium: In Honor of David Hollenbach", Eds. D. Johnstone, F. C. Adams, D. N. C. Lin, D. A. Neufeeld, & E. C. Ostriker, Astr. Soc. of the Pacific Conf. Ser. 323, p. 271
Natta, A., Grinin, V. P., Mannings, V., & Ungerechts H. 1997, ApJ, 491, 885
Okamoto, Y. K., Kataza, H., Honda, M., et al. 2004, Nature, 431, 660
Penz, T., Micela, G., & Lammer, H. 2008, A&A, 477, 309
Perrin, M. D., Graham, J. R., Kalas, P., et al. 2004, Science, 303, 1345
Pevtsov, A. A., Fisher, G. H., Acton, L. W., et al. 2003, ApJ, 598, 1387

Piètu, V., Dutrey, A., & Guilloteau, S. 2007, A&A, 467, 163
Pirzkal, N., Spillar, E. J., & Dyck, H. M. 1997, ApJ, 481, 392
Pogodin, M. A., Franco, G. A. P., & Lopes D. F. 2005, A&A, 438, 239
Pontoppidan, K. M., Dullemond, C. P., Blake, G. A., et al. 2007a, ApJ, 656, 980
Pontoppidan, K. M., Dullemond, C. P., Blake, G. A., et al. 2007b, ApJ, 656, 991
Pontoppidan, K. M., Blake, G. A., van Dishoeck, E. F., et al. 2008, ApJ, 684, 1323
Preibisch, Th., Kim, Y.-C., Favata, F., et al. 2005, ApJS, 160, 401
Preibisch, Th., Kraus, S., Driebe, Th., et al. 2006, A&A, 458, 235
Przygodda, F., van Boekel, R., Àbrahàm, P., et al. 2003, A&A, 412, L43
Reipurth, B., & Zinnecker, H. 1993, A&A, 278, 81
Roberge, A., Feldman, P. D., Lecavelier des Etangs, A., et al. 2002, ApJ, 568, 343
Royer, F., Zorec, J., & Gomez, A. E. 2007, A&A, 463, 671
Schneider, G., Smith, B. A., Becklin, E. E., et al. 1999, ApJ, 513, L127
Schneider, G., Silverstone, M. D., Hines, D. C., et al. 2006, ApJ, 650, 414
Schnerr, R. S., Rygl, K. L. J., van der Horst, A. J., et al. 2007, A&A, 470, 1105
Schütz, O., Meeus, G., & Sterzik, M. F. 2005b, A&A, 431, 175
Shu, F. H., Najita, J., Ostriker, E., et al. 1994, ApJ, 429, 781
Shu, F. H., Najita, J., Ostriker, E. C., & Shang, H. 1995, ApJ, 455, L155
Shu, F. H., Najita, J. R., Shang, H., & Li, Z.-Y. 2000, Protostars and Planets IV, 789
Shu, F. H., Shang, H., Gounelle, M., et al. 2001, ApJ, 548, 1029
Siebenmorgen, R., Natta, A., Kruegel, E., & Prusti, T. 1998, A&A, 339, 134
Siebenmorgen, R., Prusti, T., Natta, A., & Müller, T. G. 2000, A&A, 361, 258
Siess, L., Dufour, E., & Forestini, M. 2000, A&A, 358, 593
Simon, M., Dutrey, A., & Guilloteau S. 2000, ApJ, 545, 1034
Skinner, S. L., Güdel, M., Audard, M., & Smith, K. 2004, ApJ, 614, 221
Slettebak, A. 1982, ApJS, 50, 55
Sloan, G. C., Keller, L. D., Forrest, W. J., et al. 2005, ApJ, 632, 956
Stauffer, J. R., Hartmann, L. W., & Barrado y Navascues, D. 1995, ApJ, 454, 910
Stecklum, B., Eckart, A., Henning, T., & Loewe, M. 1995, A&A, 296, 463
Stelzer, B., & Neuhäuser, R. 2000, A&A, 361, 581
Stelzer, B., Micela, G., & Neuhäuser, R. 2004, A&A, 423, 1029
Stelzer, B., Micela, G., Hamaguchi, K., & Schmitt, J. H. M. M. 2006, A&A, 457, 223
Stelzer, B., Robrade, J., Schmitt, J. H. M. M., & Bouvier, J. 2009, A&A, 493, 1109
Stepien, K., & Landstreet, J. D. 2002, A&A, 384, 554
Swartz, D. A., Drake, J. J., Elsner, R. F., et al. 2005, ApJ, 628, 811
Tatulli, E., Isella, A., Natta, A., et al. 2007, A&A, 464, 55
Tatulli, E., Malbet, F., Ménard, F., et al. 2008, A&A, 489, 1151
Thé, P. S., de Winter, D., & Perez, M. R. 1994, A&AS, 104, 315
Thi, W. F., van Dishoeck, E. F., Blake, G. A., et al. 2001, ApJ, 561, 1074
Tout, C. A., & Pringle, J. E. 1995, MNRAS, 272, 528
Uzpen, B., Kobulnicky, H. A., & Kinemuchi, K. 2009, AJ, 137, 3329
van Boekel, R., Waters, L. B. F. M., Dominik, C., et al. 2004, A&A, 418, 177
van Boekel, R., Min, M., Waters, L. B. F. M., et al. 2005, A&A, 437, 189
van den Ancker, M. E., The, P. S., Tjin A Djie, H. R. E., et al. 1997, A&A, 324, L33
van den Ancker, M. E., de Winter, D., & Tjin A Djie, H. R. E. 1998, A&A, 330, 145
van der Plas, G., van den Ancker, M. E., Fedele, D., et al. 2008, A&A, 485, 487
Vieira, S. L. A., Corradi, W. J. B, Alencar, S. H. P., et al. 2003, AJ, 126, 2971
Vink, J. S., Drew, J. E., Harries, T. J., & Oudmaijer, R. D. 2002, MNRAS, 337, 356
Wade, G. A., Drouin, D., Bagnulo, S., et al. 2005, A&A, 442, L31
Wade, G. A., Bagnulo, S., Drouin, D., et al. 2007, MNRAS, 376, 1145
Walborn, N. R. 2006, In: "The Ultraviolet Universe: Stars from Birth to Death" 26th meeting of the IAU, Joint Discussion 4, 16-17 August 2006, Prague, Czech Republic, JD04, #19
Walsh, J. R. 1980, Ap&SS, 69, 227
Wassell, E. J., Grady, C. A., Woodgate, B., et al. 2006, ApJ, 650, 985
Zinnecker, H., & Preibisch, Th. 1994, A&A, 292, 152
Zuckerman, B., Song, I., Bessell, M. S., & Webb, R. A. 2001, ApJ, 562, L87
Zuckerman, B., & Song, I. 2004, ApJ, 603, 738